High-altitude electrical discharges associated with thunderstorms and lightning

Ningyu Liu[1], Matthew G. McHarg[2], and Hans C. Stenbaek-Nielsen[3]

[1]Department of Physics and Space Sciences, Florida Institute of Technology, Melbourne, FL

[2]The United States Air Force Academy, Colorado Spring, CO

[3]Geophysical Institute, University of Alaska Fairbanks, Fairbanks, AK

Corresponding author: Ningyu Liu (nliu@fit.edu), 1-321-674-7348 (phone), 1-321-674-7482 (fax)

Abstract

The purpose of this paper is to introduce electrical discharge phenomena known as transient luminous events above thunderstorms to the lightning protection community. Transient luminous events include the upward electrical discharges from thunderstorms known as starters, jets, and gigantic jets, and electrical discharges initiated in the lower ionosphere such as sprites, halos, and elves. We give an overview of these phenomena with a focus on starters, jets, gigantic jets, and sprites, because similar to ordinary lightning, streamers and leaders are basic components of these four types of transient luminous events. We present a few recent observations to illustrate their main properties and briefly review the theories. The research in transient luminous events has not only advanced our understanding of the effects of thunderstorms and lightning in the middle and upper atmosphere but also improved our knowledge of basic electrical discharge processes critical for sparks and lightning.

1. Introduction

Observation of electrical discharges above thunderstorms was first reported in the scientific literature in the late 19th century [*Lyons et al.*, 2003; *Pasko*, 2008]. It was, however, only after late 1980s and early 1990s that dedicated and systematic scientific studies by using modern optical detectors, radio instruments and computer modeling tools started to reveal their physical properties and origins [e.g., *Franz et al.,* 1990; *Inan et al.,* 1991; *Sentman et al.,* 1995; *Wescott et al.,* 1995; *Pasko et al*., 1997]. They are one of the research subjects actively pursued by the research community of atmospheric and space electricity and are normally referred to as transient luminous events [e.g., *Pasko,* 2010; *Liu,* 2014]. Transient luminous events come with a variety of forms and are categorized as starters, jets, gigantic jets, sprites, halos, and elves. They differ in morphology, time duration, home layer of the atmosphere, physical mechanism, etc. Nonetheless, they are all related to thunderstorm/lightning activities at tropospheric altitudes and manifest direct electrical coupling between tropospheric thunderstorms and the middle and upper atmosphere.

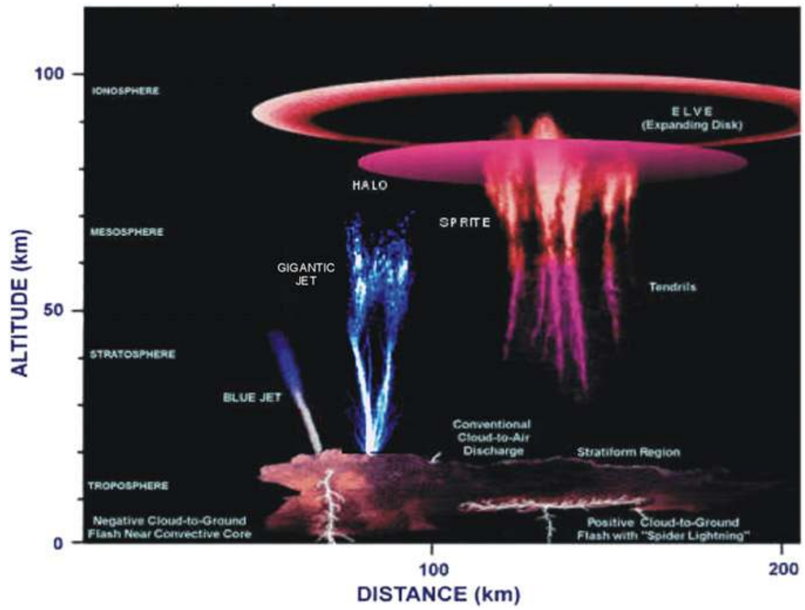

Figure 1. Transient luminous events caused by thunderstorm/lightning activities [*Stenbaek-Nielsen et al.*, 2013]. The figure is adapted from [*Lyons et al.,* 2000], illustrating typical features of transient luminous events present in video observations.

Figure 1 shows the appearances, and the horizontal and vertical extents of a few forms of transient luminous events. Starters (not shown in Figure 1), jets, and gigantic jets are upward electrical discharges from thunderstorms [e.g., *Wescott et al.,* 1995, 1996, 2001a; *Pasko et al.,* 2002, 2003; *Lyons et al.,* 2003; *Su et al.,* 2003; *Neubert,* 2003; *Pasko*, 2008; *Krehbiel et al.,* 2008; *Liu et al.,* 2015]. Their tops reach different altitudes: 20-30 km for starters, 40-50 km for jets, and 70-90 km for gigantic jets. Starters and jets typically appear as a cone of blue light shooting upward from thunderstorms with a dimmer fan near their tops [e.g., *Wescott et al.,* 1995, 1996, 2001a; *Lyons et al.,* 2003; *Edens*, 2011; *Chou* et al., 2011; *Suzuki* et al., 2012; *Liu et al.,* 2015]. Gigantic jets, on the other hand, have a tree-like structure and display more complex dynamics [e.g., *Pasko et al.,* 2002, *Su et al.,* 2003; *Chou et al.,* 2010; *Soula et al.,* 2011; *Liu et al.,* 2015]. The top of gigantic jets reaches earth's ionosphere, and they can rapidly transfer a large amount of charge between thunderstorms and the ionosphere [*Cummer et al.,* 2009; *Kuo et al.,* 2009; *Lu et al.,* 2011; *Liu et al.,* 2015]. Among transient luminous events, starters, jets, and gigantic jets are the closest kin of ordinary lightning, because they share the same underlying discharge process, leaders.

Sprites are large, luminous electrical discharges in the upper atmosphere caused by intense cloud-to-ground lightning flashes [*Franz et al.,* 1990; *Sentman et al.,* 1995; *Pasko et al.,* 1997]. They were theoretically predicted by Nobel Prize Laureate C.T.R. Wilson in 1925 [*Wilson*, 1925]. Their dynamics are governed by streamer discharges [e.g., *Pasko et al.,* 1998; *Liu and Pasko*, 2004; *Ebert et al.,* 2006; *Liu et al.,* 2009a,b; *Luque and Ebert,* 2009, 2010; *Pasko et al.,* 2013; *Liu*, 2014]. Sprites are typically initiated at 70-85 km altitudes with downward propagating streamers, which terminate at about 40-50 km altitudes [e.g., *Stanley et al.,* 1999; *Stenbaek-Nielsen et al.,* 2000; *Cummer et al.,* 2006; *McHarg et al.,* 2007; *Stenbaek-Nielsen et al.,* 2007, 2010, 2013; *Stenbaek-Nielsen and McHarg,* 2008]. Upward propagating streamers may appear later and can reach about 90 km altitude [*Stanley et al.,* 1999; *Cummer et al.,* 2006; *McHarg et al.,* 2007; *Stenbaek-Nielsen et al.,* 2007, 2010, 2013; *Stenbaek-Nielsen and McHarg,* 2008]. In Sections 2 and 3, we discuss starters, jets, gigantic jets, and sprites in more detail, because similar to ordinary lightning, streamers and leaders dominate their dynamics.

Halos are a homogeneous glow that typically appears within 1-2 ms after an intense CG stroke and lasts for several milliseconds [e.g., *Stenbaek-Nielsen et al.,* 2000; *Barrington-Leigh et al.,* 2001; *Wescott et al.,* 2001b; *Miyasato et al.,* 2002; *Newsome and Inan,* 2010]. Typical halos are centered around 75-80 km altitude with a horizontal extent of tens of kilometers and vertical thickness of several kilometers. They may occur as an isolated event or may be preceded by elves and/or followed by sprites. Intense CG strokes of both positive and negative polarities can effectively cause halos [e.g., *Williams,* 2006; *Frey et al.,* 2007; *Williams et al.,* 2007; *Taylor et al.,* 2008; *Newsome and Inan,* 2010; *Williams et al.,* 2012; *Li et al.,* 2012].

Elves are a fast expanding ring of optical emissions in the lower ionosphere induced by lightning discharges. Similar to sprites, elves were theoretically predicted before their experimental documentation was published in scientific literature. *Inan et al.* [1991] found that the electromagnetic field pulses radiated by CGs can heat the electrons in the lower ionosphere at 90-95 km altitudes to sufficient energies to excite and ionize neutral molecules. This can result in a brief enhancement of airglow, which is now called elves, an acronym for Emissions of Light and VLF perturbations due to EMP Sources [*Fukunishi et al.,* 1996]. Figure 1 includes an elve that looks like a thin ring. Compared to halos, they occur at a slightly higher altitude, ~90 km, appear earlier by about 100-200 μs, and last for a shorter period of time (<1 ms) [*Barrington-Leigh et al.,* 2001; *Newsome and Inan,* 2010]. Given that both elves and halos appear as brief diffuse glows in the lower ionosphere, it is generally difficult to differentiate one against the other with video recordings of standard TV frame rates or even slightly higher [*Barrington-Leigh et al.,* 2001; *Newsome and Inan,* 2010].

Elves expand at an apparent speed greater than the speed of light, and their lateral extent can reach a few hundreds of kilometers [*Inan et al.,* 1996; 1997]. Their appearance depends on the viewing geometry [*Inan et al.,* 1996; 1997; *Kuo et al.,* 2007; *Marshall et al.,* 2010; *Marshall,* 2012]. When viewed upward from above thunderstorms, an elve appears as a ring, which is also known as the doughnut shape of the elve. The minimum intensity at the center of the ring is due to the minimum in the radiated EMP intensity above the source lightning current. When viewed from a slanted direction on ground, the rapid horizontal expansion of the luminous ring results in apparent downward motion of the elve.

According to the survey from the Imager of Sprites and Upper Atmospheric Lightning (ISUAL) experiment aboard the FORMOSAT-2 satellite [e.g., *Chern et al.,* 2004; *Mende et al.*, 2005], the global occurrence rates of elves, sprites, halos, and gigantic jets are 3.23, 0.5 0.939, and 0.01 events per minute, respectively [*Chen et al.,* 2008]. When the instrumental effects and the area coverage of the survey are taken into account, the global occurrence rates of sprites and elves are expected to increase by a factor of two and a factor of ten, respectively [*Chen et al.,* 2008].

Transient luminous events are driven by the electric field of thundercloud charge and lightning. The occurrence of starters, jets, and gigantic jets is normally associated with suddenly increased lightning activities in a short time window on the order of seconds [e.g., *Wescott et al.,* 1998; *Suzuki et al.,* 2012;

Liu et al., 2015]. They are not coincident with a particular cloud-to-ground (CG) lightning stroke [e.g., *Wescott et al.,* 1998; *Su et al.,* 2003, *Cummer et al.,* 2009; *Edens,* 2011; *Lu et al.,* 2011; *Soula et al.,* 2011; *Suzuki et al.,* 2012; *Liu et al.,* 2015], but preceding CGs can create electrical conditions that promote their formation [e.g., *Krehbiel et al.,* 2008; *Riousset et al.,* 2010a; *Edens,* 2011]. Normal intra-cloud (IC) lightning discharges can also create favorable conditions for their formation [*Krehbiel et al.,* 2008; *Riousset et al.,* 2010a; *Lu et al.,* 2011; *Liu et al.,* 2015], and in fact, the upward electrical discharges sometimes begin as part of normal IC flashes [*Lu et al.,* 2011; *Liu et al.,* 2015]. On the other hand, elves, halos, and sprites are caused by intense CGs. As mentioned above, elves are the result of ionospheric electrons accelerated by the electromagnetic field pulses emitted by CGs, and they appear within 1 ms from the CGs. The peak current of a CG stroke is the most important parameter to gauge if it will cause an elve [*Inan et al.,* 1996; 1997; *Kuo et al.,* 2007; *Marshall et al.,* 2010; *Marshall,* 2012]. Halos and sprites are the products of the excitation and ionization of air molecules due to collisions with electrons accelerated by the quasi-electrostatic field (QE) established in the upper atmosphere by the CG and its possible continuing current [e.g., *Pasko et al.,* 1997; *Barrington-Leigh et al.,* 2001; *Li et al.,* 2008]. The magnitude of the QE field is mainly determined by the amount of the charge removed by the CG and the altitude from which it is removed [e.g., *Pasko et al.,* 1997; *Cummer and Inan,* 1997; *Cummer et al.,* 2013]. Halos typically appear a few milliseconds later after the CGs, and the delay of sprites from the CGs can vary from a few milliseconds to tens or hundreds of milliseconds. If all three phenomena are triggered by a CG, elves will come first, then halos, and finally, sprites.

Two important factors determining the dynamics of transient luminous events are the magnitude of electric field and its duration at the corresponding atmospheric regions. The accelerated electrons leading to transient luminous events gain energy from electric field and lose energy via collisions with neutrals. Air density, which determines the collision frequency in large part, is therefore an important parameter. On the other hand, the duration of the electric field depends on the atmospheric conductivity. Figure 2 shows the altitude profiles of air density and atmospheric conductivity from 0 km to 100 km altitude. The air density approximately decreases exponentially with the altitude. The atmospheric conductivity profile is broken down into two regions: the ion conductivity dominating region (<~65 km) and the electronic conductivity dominating region (>~65 km). The duration of the electric field at a particular altitude is roughly equal to the local Maxwellian relaxation time (ε_0/σ, where σ is the local conductivity and ε_0 is the permittivity of free space) [*Pasko et al.,* 1997]. The local Maxwellian relaxation time calculated by using the conductivity shown in Figure 2 is <1 ms above 80 km altitude, 1-10s ms at 70 km, and ~1 s at 30 km, which characterize the lifetimes of the electrical discharge phenomena at those altitudes: <1 ms for elves, ~2 ms for halos, 1-10s ms and occasionally 100s ms for sprites, and 100s ms for jets and gigantic jets. It should be mentioned that the ionospheric conductivity profile between 60 and 90 km altitudes varies significantly from day to night and from low latitudes to high latitudes. The profile shown in Figure 2 is only one of a few typical profiles used in the studies of transient luminous events.

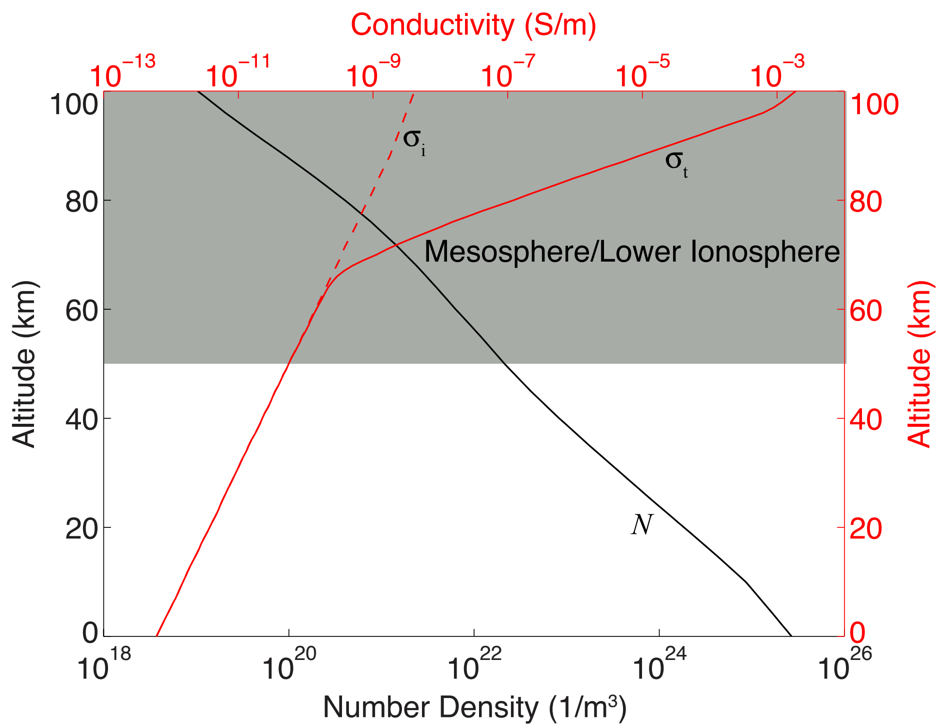

Figure 2. Altitude profiles of neutral density and conductivity [*Liu*, 2012]. The neutral density profile is obtained from the MSIS model (http://omniweb.gsfc.nasa.gov/vitmo/msis_vitmo.html). The ion conductivity σ_i is taken from [*Holzworth et al.,* 1985]. The electron density to calculate the electronic conductivity is taken from [*Wait and Spies*, 1964*; Pasko and Stenbaek-Nielsen*, 2002]. The total conductivity σ_t is dominated by the ion component below ~65 km altitude and by the electronic component above that altitude.

A large body of literature has been published in the research field of transient luminous events. Many recent papers reviewed the current state of this field [*Pasko,* 2010; *Inan et al.,* 2010; *Ebert et al.,* 2010; *Pasko et al.,* 2011, 2013; *Stenbaek-Nielsen et al.,* 2013; *Liu*, 2014], and papers published in journal special issues or sections [*Ebert and Sentman,* 2008; *Sentman,* 2010; *Gordillo-Vázquez and Luque,* 2013] presented recent studies on different aspects of transient luminous events. Detailed discussion of earlier work in this field can be found in the book edited by *Füllekrug et al.* [2006], and earlier review papers [e.g., *Pasko,* 2007*,* 2008; *Neubert et al.,* 2008; *Stenbaek-Nielsen and McHarg,* 2008]. Interested readers are referred to those publications. In the sections below, we present a few observations of starters, jets, gigantic jets, and sprites to illustrate their main properties and to show how the research work in this field advances our understanding of basic electrical discharge processes in air.

2. Starters, jets, and gigantic jets

2.1 Overview

In contrast to frequent occurrences of cloud-to-ground lightning strokes during thunderstorms, upward electrical discharges from thunderstorm tops are rare, and only a limited number of reports of their observation exist in the scientific literature [e.g., *Lyons et al.*, 2003; *Pasko*, 2008; *Meyers et al.*, 2013]. The meteorological conditions of the storms producing them have been investigated by several studies, but it is unclear why the upward electrical discharges are so rare [e.g., *Lyons et al.,* 2006; *van der Velde et al.,* 2007*,* 2010; *Meyers et al.,* 2013].

Starters and jets are upward electrical discharges from thundercloud tops reaching about 25 km and 40 km altitude, respectively. The starters and jets reported by different studies share common main features in temporal and spatial properties but may differ in details [*Wescott et al.,* 1995*,* 1996, 2001a; *Lyons et al.,* 2003; *Chou et al.,* 2011; *Suzuki et al.,* 2012; *Liu et al.,* 2015]. Their principal properties are depicted by a series of papers published by Wescott and his colleagues [*Wescott et al.,* 1995*,* 1996*,* 1998, 2001a], who analyzed the results obtained from a few observation campaigns including the successful Sprites94 aircraft campaign. The starters and jets observed in the Sprites94 campaign occurred in two very active thunderstorm cells, with an unusually large lightning flash rate of 200-300 flashes/min, in the Midwest of United States. A total of 51 jets that appeared as narrow cones of blue light shooting upward from the tops of thunderstorms were recorded from a distance of 100 km or so [*Wescott et al.,* 1995]. They originated from an average altitude of 17.7 km and reached 37.2±5.3 km. Few of them developed in the vertical direction, and the mean angle between the propagation direction and the vertical was 10.8°±7.0°. The average angle of the luminous cone of the jet was 14.7°±7.5°. Note that the number following each mean value represents the range of the parameter not the error. The lifetime of a jet varied from 200 to 300 ms. Starters with a terminal altitude ranging from 18.1 to 25.7 km were also recorded during this campaign [*Wescott et al.,* 1996]. They originated from a similar altitude as the jet [*Wescott et al.,* 1996], and their speeds varied in a wide range from 27 km/s to 153 km/s.

The connection between the activities of ordinary lightning flashes and jets/starters has been investigated in detail by the studies reporting observation of many jet and starter events from a single storm. It was found that the lightning flash rates of both CGs [e.g., *Wescott et al.,* 1995, 1996, 1998; *Suzuki et al.,* 2012] and ICs [*Suzuki et al.,* 2012] suddenly increased 1 s before the jets and then quickly decreased afterward. Although the CG activities displayed the same pattern for the starter events [e.g., *Wescott et al.,* 1995, 1996, 1998; *Suzuki et al.,* 2012], the IC flashes were very active within ±1 s time window from the starters [*Suzuki et al.,* 2012]. The flash rate within 30 km from jets was about 25 percent higher than the rate within the same distance from starters, suggesting that more charge was transferred to ground before the jets than before the starters [*Wescott et al.,* 1995, 1996, 1998]. It was also found that neither jets nor starters were coincident with a particular CG flash [*Wescott et al.,* 1995, 1996, 1998], but the correlations with the lightning rates may indicate that the jets were strongly connected with –CGs, and starters were more affected by ICs [*Suzuki et al.,* 2012]. The charge moment changes within ±1 s of jets/starters were on the order of -100-200 C km, and assuming that charge was removed from an altitude of 8 km, the corresponding charge transferred was about -12.5 C to -25 C [*Suzuki et al.,* 2012]. In addition, the peak of the distribution of the histogram of the time interval between two successive jets was 60-70 s, while the same peak for the starters was less than 5 s [*Suzuki et al.,* 2012].

The in-cloud electrical breakdown processes initiating/accompanying a jet [*Krehbiel et al.,* 2008] and a starter [*Edens,* 2011] have been mapped by a three-dimensional very high-frequency (VHF) lightning mapping array (LMA) [*Rison et al.,* 1999] that is efficient at detecting negative breakdown during thunderstorms [*Krehbiel et al.,* 2008]. According to LMA data, both events were initiated midway between the upper cloud charge and the cloud top screening charge. The electrical breakdown process began about 10 s after an intracloud discharge selectively neutralized positive cloud charge in the volume right below the initiation location of the jet [*Krehbiel et al.,* 2008]. The starter occurred during an NLDN (U. S. National Lightning Detection Network) negative CG flash of 7 strokes [*Edens,* 2011]. The LMA data showed that the starter originated as a bidirectional discharge at ~14 km altitude. The positive discharge propagated upward, exited the top of the cloud at 15.2 km altitude, and was observed optically as the starter. The downward negative discharge extended into the positive charge region but the associated LMA sources associated were only observed in a relatively localized volume, indicating only a small amount of positive cloud charge was tapped into by the negative discharge. The author suggested this was probably the reason why the starter did not evolve into a full-scale jet.

Gigantic jets were first discovered in September 2001 over an oceanic thunderstorm near the Arecibo Observatory, Puerto Rico [*Pasko et al.,* 2002]. They are electrical discharges originating in cloud tops and extending upward to lower ionospheric altitudes of 70-90 km [*Pasko et al.,* 2002; *Su et al.,* 2003; *Pasko,* 2003]. They can rapidly transfer a large amount of charge between thunderstorms and the conducting ionosphere [*Su et al.,* 2003; *Cummer et al.,* 2009; *Kuo et al.,* 2009; *Lu et al.,* 2011; *van der Velde et al.,* 2010; *Liu et al.,* 2015]. Gigantic jets mainly occur above tropical or tropical-like storms [*Chen et al.,* 2008, *Chou et al.,* 2010; *van der Velde et al.,* 2010; *Meyer et al.,* 2013]. The altitude of the top of the parent cloud is typically greater than 15 km [e.g., *Meyer et al.,* 2013]. A noticeable exception is a winter storm with a cloud top altitude of 6-7 km [*van der Velde et al.,* 2010]. They occur predominately in tropical and subtropical regions, but have also been observed at high latitudes of 35.6-42°N [*van der Velde et al.,* 2010; *Yang and Feng,* 2012]. They typically have a tree-like structure [*Pasko et al.,* 2002; *Su et al.,* 2003; *Soula et al.,* 2011; *Liu et al.,* 2015]. The color images show that the lower part (~20-40 km altitude) of gigantic jets is bluish, the upper part (> 65 km) is red, and a color transition zone spans between those two regions [*Soula et al.,* 2011]. Compared to other TLEs, they are rare, but similar to other TLEs, multiple gigantic jets can be produced by a single storm [*Su et al.,* 2003; *Soula et al.,* 2011; *Huang et al.,* 2012; *Liu et al.,* 2015].

Gigantic jets are not associated with a particular CG flash but are connected to intracloud discharge activities [*Su et al.,* 2003, *Cummer et al.,* 2009; *Lu et al.,* 2011; *Soula et al.,* 2011; *Liu et al.,* 2015]. The accompanying cloud flashes are clearly visible in the videos recorded from a close distance [*Soula et al.,* 2011; *Liu et al.,* 2015]. For the seven upward electrical discharges (one starter, two jets, and four gigantic jets) observed above Tropical Depression Dorian [*Liu et al.,* 2015], NLDN IC event rate suddenly increased in a short time interval of 1-2 s containing each event, and CG activity was detected by NLDN only for one of the gigantic jet events. The in-cloud discharges initiating/accompanying gigantic jets have also been investigated in detail by using VHF lightning mapping networks [*Lu et al.,* 2011]. Two negative gigantic jets from two different storms were analyzed, and both of them occurred as part of flashes that began as ordinary intracloud lightning. For both events, the data show that two distinct upward negative leaders developed sequentially. The first leader propagated into the upper positive cloud charge layer and resulted in many detections by the LMA system. The second leader was initiated about 100 ms after the first leader stopped propagation. Then it penetrated through the cloud top and developed into gigantic jets. The authors suggested that this specific discharge development might have created conditions more favorable for an upward negative leader to escape the cloud vertically.

The upward electrical discharges can be of either positive or negative polarity depending on the polarity of the initiating upward leader. For normal polarity storms (i.e., the main positive charge layer of the storm resides over its main negative charge layer), if the initiating upward leader begins between the main negative charge and the upper positive charge, the resulting event is of negative polarity; if it begins between the upper positive charge and the cloud top screening charge, the resulting event is of positive polarity. If the storm is of inverted polarity, the polarity of the event is reversed.

In the sections below, we first review the current theory of the upward electrical discharges, and then discuss a few upward electrical discharge events observed above Dorian in September 2013 from a close distance [*Liu et al.,* 2015] to illustrate their basic properties in more detail.

2.2 Theory

2.2.1 Formation of upward electrical discharges

Krehbiel et al. [2008] and *Riousset et al.* [2010a] proposed a unifying view of how electrical discharges originating inside thunderstorms escape to form cloud-to-ground lightning, bolt-from-the-blue discharges, jets, or gigantic jets. According to this theory, in order for an electrical discharge originating inside a thunderstorm to escape from it, a charge imbalance condition in the thunderstorm (either globally or locally) must be created by electrical or meteorological processes. There are two principal mechanisms for creating the upward electrical discharges from thunderstorms. Consider the standard model of the charge structure of thunderstorms that consists of two cloud charge layers of opposite polarities centered at different cloud altitudes and a screening charge layer around the cloud top, which has the same polarity as the lower cloud charge. The upward electrical discharges can be developed from electrical breakdown beginning either between the two cloud charge layers or between the upper cloud charge and the screening charge, where electric field is typically strongest. If a proper charge imbalance condition exists, the initiated upward electrical discharge can penetrate through the charge layer it is directed to, and escape from the cloud top. Because the directions of the electric field are opposite at those two regions, the resulting upward electrical discharges have different polarities. This theory has been verified by observations reported later indicating that the upward discharges beginning between the upper cloud charge and the screening charge tend to develop into starters or jets [*Edens*, et al., 2011], while those beginning between two cloud charge layers evolve into gigantic jets [e.g., *Cummer et al.,* 2009; *Lu et al.,* 2011].

An example of the electrical processes for creating the required charge imbalance condition to produce upward discharges is a CG stroke. For normally electrified thunderstorms that are charged negatively (see detailed discussion in [*Riousset et al.,* 2010a]), negative CGs can suddenly change the charge polarity of the thunderstorms and make it possible for an initiated upward positive discharge between the upper positive charge layer and the screening charge to escape from the cloud tops. According to fractal modeling results, the escaped discharges tend to develop into jets.

On the contrary, when the positive charge of normally electrified thunderstorm is depleted due to mixing with the screening charge, an upward negative discharge as part of an intracloud flash (i.e., initiated between the main negative charge and the upper positive charge, or positive IC) may continue propagating upward upon reaching the cloud top, and form gigantic jets. In this sense, gigantic jets share a very similar scenario of development as more familiar “bolt-from-the-blue” lightning discharges that instead of propagating upward to exit the cloud, the discharge originating inside the cloud exits sideways and turns downward to ground [*Krehbiel et al.,* 2008; *Riousset et al.,* 2010a]. According to this theory, jets are of positive polarity and gigantic jets are of negative polarity for normally electrified thunderstorms; for thunderstorms with inverted polarity, the polarity is reversed.

Note that according to *Liu et al.* [2015], not every upward leader originating between the main cloud charges and successfully escaping upward into space develops into a gigantic jet.

2.2.2 Leaders in upward electrical discharges

The underlying electrical discharge process driving the development of starters, jets, and gigantic jets is leaders [*Petrov and Petrova*, 1999; *Raizer et al.,* 2006*,* 2007; *Krehbiel et al.,* 2008; *Riousset* et al., 2010a, b; *da Silva and Pasko*, 2012, 2013a, b, *Liu et al.,* 2015], similar to ordinary lightning. Leader discharges are responsible for electrically breaking down air to form a hot (>5000 K), highly conductive channel, and their initiation and propagation mechanisms are not well understood at present. Meter-long leaders can be generated and studied in laboratory experiments. However, the kilometer-long leaders of natural electrical discharges possess significantly different characteristics, because the involved spatial and temporal scales are much larger and there are no well-defined counterparts to the electrodes and discharge gaps of laboratory experiments.

That leaders must be the principal discharge process for the upward electrical discharges is concluded based on the following considerations. First, cold plasma channels created by electrical discharges like streamers can only maintain their conductivity on a timescale of a few microseconds at thundercloud top altitudes. They are unable to sustain a channel current to support the development of starters, jets, and gigantic jets on a timescale of tens or hundreds of milliseconds [*Raizer et al.,* 2006*,* 2007]. Second, the propagation characteristics, such as speed, current, linear charge density, and luminosity, of the channels of starters, jets, and gigantic jets are similar to leaders' [*Pasko et al.,* 2002, *Su et al.,* 2003; *Soula et al.*, 2011; *Liu et al.,* 2015]. Third, theoretical and modeling studies of the streamer-to-leader transition timescale and leader speed at higher altitudes give values not inconsistent with the characteristic time scale of the propagation of the upward electrical discharges [*Riousset* et al., 2010b; *da Silva and Pasko*, 2012, 2013a, b].

There are, however, notable differences in the properties between the leaders of the upward electrical discharges and ordinary lightning. The streamer-to-leader transition requires a much longer timescale or it takes a significantly longer timescale to create a new section of the leader channel. This timescale is inversely proportional to the squared of air density [*Riousset* et al., 2010b; *da Silva and Pasko*, 2012, 2013a, b]. The streamer-to-leader transition time depends on the leader radius and the current carried by the leader. For a typical leader (with a radius of 0.3 mm at ground or 10 cm at 40 km altitude) carrying a current of 100 A, the transition occurs on the order of 10 ns at ground pressure, but takes about 1 ms at 40 km altitude [*Silva and Pasko*, 2013b]. In contrast to the negative stepping leaders of ordinary lightning, the leaders of the upward electrical discharges give no radiation in the low frequency (LF) band [*Liu et al.,* 2015]. The absence of LF activities suggests that the stepping of the negative leader above thunderclouds occurs on a longer timescale, possibly resulting from a larger spatial scale of the discharge at higher altitudes, as suggested by the scaling laws of electrical discharges in air [*Pasko*, 2006; *Liu,* 2014].

2.3 Phenomenology of Dorian events

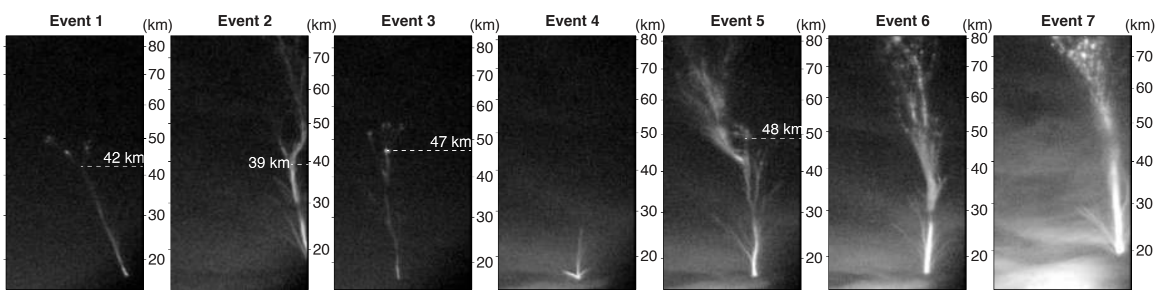

Figure 3. Low-light-level video fields of seven upward discharges observed above Tropical Depression Dorian over the Atlantic Ocean on 3 August 2013 [*Liu et al.,* 2015]. Events 1 and 3 are jets, event 4 is a starter, and the rest of the events are gigantic jets.

Seven upward electrical discharge events above Tropical Depression Dorian over the Atlantic Ocean were recorded from a distance of 80 km between

3:45 UTC and 4:12 UTC on 3 August 2013 [*Liu et al.,* 2015]. The images shown here are cropped video fields (16.7 ms exposure) that are extracted from the videos recorded by a low-light-level TV camera with a standard frame rate of 29.97 fps. Figure 3 shows the seven events at the moments when they are fully developed. Events 1 and 3 are jets, and their terminal altitudes are 51 and 55 km, respectively; events 2, 5, 6, and 7 are gigantic jets, and their tops are outside the field of view of the camera, giving terminal altitudes greater than 77-82 km; event 4 is a starter and terminates at about 26 km altitude. The images show that all of the events have a tree-like structure.

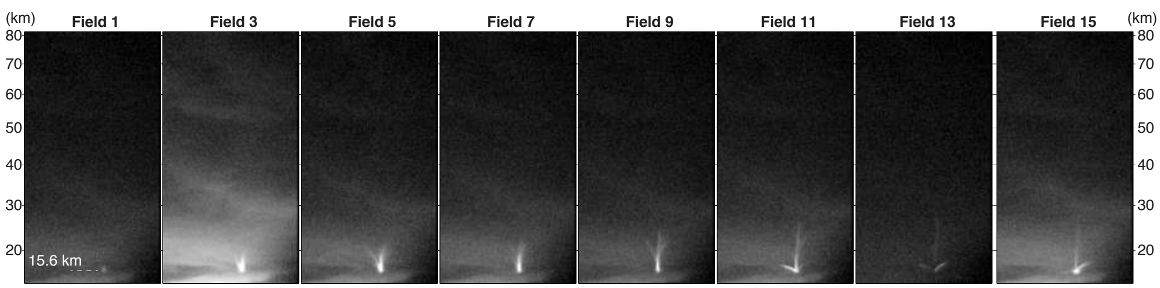

Figure 4. Selected video fields of the starter (event 4).

Figures 4-7 show the detailed temporal dynamics of the starter (event 4), a jet (event 1), and two gigantic jets (events 5 and 7). The starter lasted about 260 ms and had multiple branches connecting to a common, bright base.

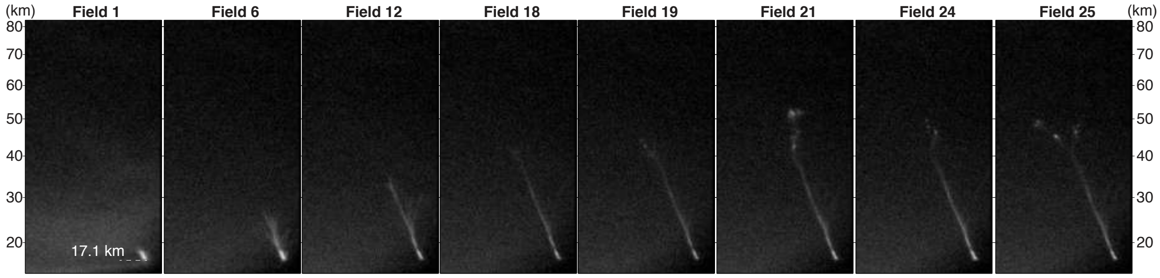

Figure 5. Selected video fields of a jet (event 1).

Figure 5 shows event 1 started with an upward propagating leader, which has a single main channel tilting from the vertical with an angle of about 21 degrees. For the next ~270 ms (16 video fields), the leader continued moving in that direction, while constantly spawning dimmer channels in a narrow cone of about 30 degrees. When it reached 42 km altitude (fields 17 and 18), the leader appeared unable to continue its steady propagation, and dimmer channels originated from its top simultaneously and sequentially, as shown in the fields from 19 to 25. In field 19, a short, hardly visible vertical channel extended upward from the leader tip, it disappeared in the next field, and then a small tree-like structure with a relatively larger vertical and horizontal extent suddenly appeared in field 21. After field 25, the luminosity of the entire leader channel decreased rapidly and completely vanished in 4 video fields. The dynamics of the other jet (event 3) were very similar, and the main leader reached about 47 km altitude before it stopped extending upward and generated multiple branches at its tip.

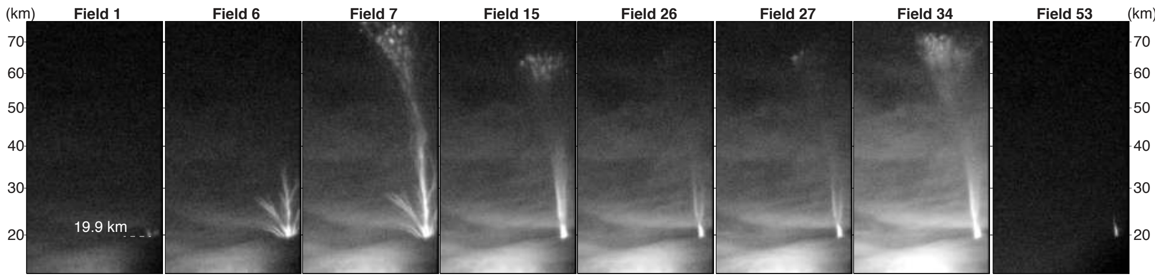

Figure 6. Selected video fields of a gigantic jet (event 7).

Figure 6 shows the development of event 7, a gigantic jet, which is the most impulsive event among the seven events. The leader emerged from the cloud top with several distinct branches, but the center branch had the highest top. It reached 34.8 km altitude in field 6, and then jumped to >77.1 km altitude in the next video field. After the jump, relatively stationary bright beads and dimmer glows appeared at the top of the discharge. The luminosity of the top gradually decayed afterwards, while bead-like structures with short trails moved upward from about 50 km altitude along the preexisting channels, as shown in field 15. The luminosity continued to decrease until field 26, when the top of the gigantic started to rebrighten as well as the scattered light from cloud lightning activity. The rebrightening reached its strongest stage in fields 34 and 35, which lasted 7 fields, and upward motion of the beads at the top is visible as well as horizontal displacement of the entire discharge volume. After the main body of the gigantic jet vanished, a short bright column base above the cloud, as shown in field 53, persisted for a while, and the entire duration of the discharge was as long as 1.2 s. This is probably the longest duration of the upward cloud discharges that have ever been reported. The upward propagation of event 6 was very similar, but no rebrightening occurred for this gigantic jet after the discharge reached the ionosphere.

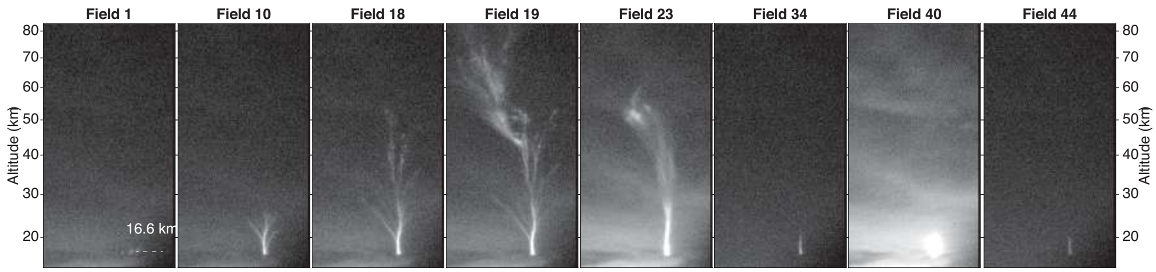

Figure 7. Selected video fields of a gigantic jet (event 5).

The gigantic jets 2 and 5, however, initially propagated upward similarly like the jets, as shown by Figure 7. When they reached 39 and 48 km altitudes, respectively, multiple branches were produced at their tops like the jets, and then in the next video field, one of those branches (event 2) or a branch below the top (event 5) made the final jump. Both events were followed by an intense lightning flash, which seems to fuel the short bases of the upward discharges to emit extremely bright light. This can be clearly seen in field 40 in Figure 7.

2.4 Electrical discharge characteristics

2.4.1 Speed

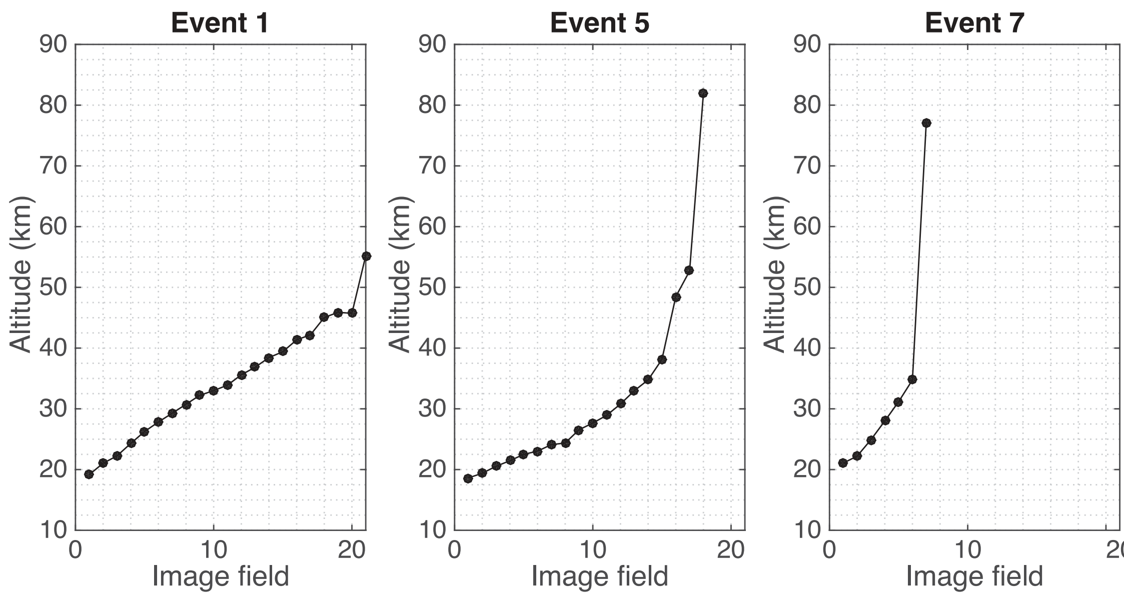

Figure 8. The altitudes of the tops of a jet (event 1) and two gigantic jets (events 5 and 7). The horizontal axis shows the image field number. Note that the horizontal and vertical axes have the same ranges in all three panels.

Figures 8 and 9 show the altitudes and vertical speeds of the tops of a jet (event 1) and two gigantic jets (event 5 and 7). As shown by the figures, the speed of the upward leaders of all three events is on the order of 10^5 m/s before they almost reach their full extents. However, the speed of the jet leader shows a slight decrease over an extended time period (i.e., from the beginning to image field 15), while the speeds of the gigantic jets leaders increase. The vertical speed of event 7 is initially 6.8×10^4 m/s, and then increases from 1.6×10^5 to 2.1×10^5 m/s. The final jump of the leader to reach the ionosphere corresponds to a speed greater than 2.5×10^6 m/s. The jet event indicates even if an upward leader reaches a relatively high altitude, it may not make the final jump to reach the ionosphere. On the other hand, events 5 and 7 show that the final jump of gigantic jets can be made at different altitudes. Consistently, the duration of the upward propagation stage before the final jump varies.

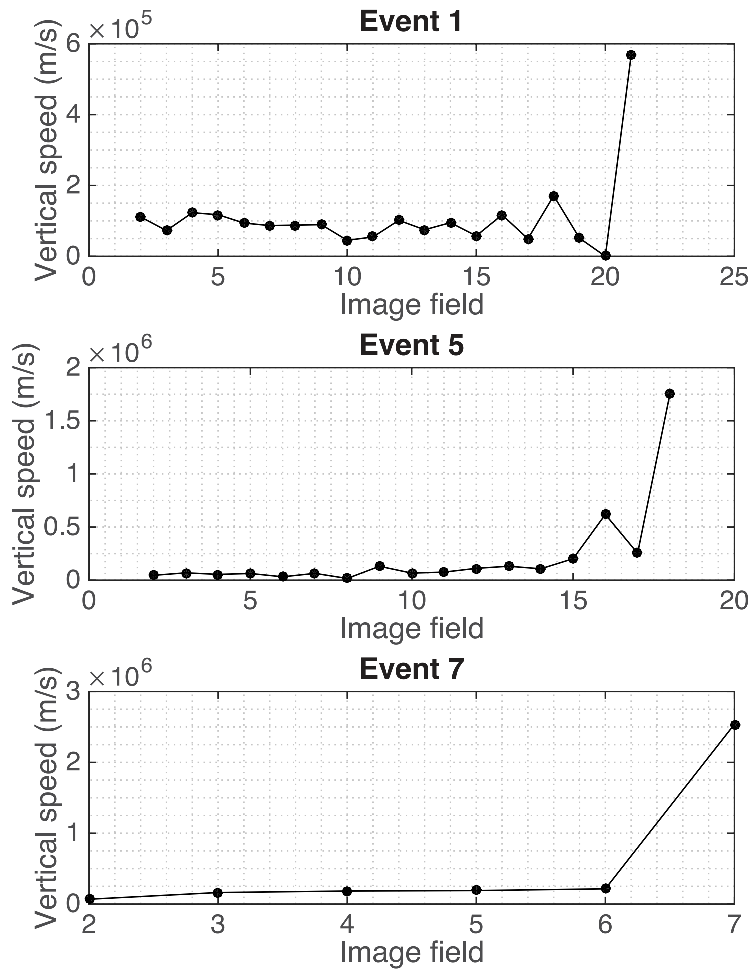

Figure 9. The vertical speeds of the tops of a jet (event 1) and two gigantic jets (events 5 and 7).

2.4.2 Charge and current

The information of the current flowing along the upward electrical discharge can be inferred from remote measurements of the ultra-low-frequency radio emission radiated by the discharge [*Cummer et al.,* 2009; *Liu et al.,* 2015]. The parameter directly found from the measurement is current moment that is the integral of the current over the entire discharge channel. The charge moment change can then be obtained by integrating the current moment over the discharge period.

The current moment of event 1 varies in a range of 1.5-2.5 kA-km during its steady upward propagation. Assuming a 25 km vertical channel, the current varies from 60 to 100 A [*Liu et al.,* 2015]. As the discharge propagates upward, the current moment gradually decreases, so the current decreases given that the channel length increases. When its tip reaches 42 km altitude, the current is about 25 A, assuming that the lower end of the discharge is at 13 km altitude. The measured total charge moment change due to the event is 0.98 kC km, corresponding to 56 C charge transfer if the channel is assumed to be uniformly charged and have a length of 35 km. Since there is only a single leader channel, the linear charge density of the channel can be readily estimated and the obtained value is about 1.5 mC/m, which is consistent with the linear charge density of a lightning leader [*Rakov and Uman,* 2003, p. 123-126].

The total charge moment change caused by event 7 is approximately 8.7 kC-km, and the total deposited charge in the middle and upper atmosphere is about 134 C assuming a channel length of 65 km [*Liu et al.,* 2015]. The initial current moment before the final jump is slightly larger than the value of event 1, and the resulting charge moment change is about 0.4 kC-km, comparable to the 0.98 kC km value of event 1. During the final jump, the current moment of the gigantic jet rapidly increases to 40 kA-km. The current moment maintains at this high level for 30 ms, and then decreases to 20 kA-km and stays there for the next 160 ms. About 65% (85 C) of the total amount of charge transferred between the thunderstorm and the ionosphere by this event occurs during this approximately 200 ms period. The rebrightening is accompanied by an increase in the current flowing in the discharge channel, resulting in a charge moment change of 1.8 kC-km (21% of the total charge moment change of the event). The other gigantic jets (without rebrightening) have similar current moment and charge moment waveforms up to the moment of rebrightening, with the charge moment change before the final jump varying in the range of 0.3-1 kC-km [*Liu et al.,* 2015].

2.4.3 Leader streamer zone size and leader potential

After the leader of the event 1 reached 42 km altitude, the discharges at the leader tip differed from the leader in the spatial structures and temporal dynamics. It is reasonable to speculate that they manifest the streamer zone preceding the leader tip. If this is true, the vertical extent of the streamer zone is about 11 km for this particular leader tip at 42 km altitude. For gigantic jets, the accepted view is that the streamer zone extends from the tip of the leader right before the final jump up to the ionosphere [*Raizer et al.,* 2006*,* 2007; *da Silva and Pasko*, 2013a, b]. The streamer zone extends upward from approximately 35 km altitude for event 7 and approximately 45 km altitude for event 5. Therefore, the streamer zone size can vary significantly for the leader at high altitude, but the leader tip potential does not vary as significantly as the streamer zone size because the streamer zone field is believed to decrease exponentially as altitude increases.

From the leader theory, the electric potential difference between the leader tip and the ionosphere can be determined if its altitude and streamer zone size are known, assuming that the electric field in the streamer zone is the critical field for streamer propagation [*Raizer et al.,* 2006*,* 2007; *da Silva and Pasko*, 2013a, b]. For event 1, if this field is assumed to be the critical field for negative streamer propagation, which is about 2-3 times larger than that field for positive streamers, the current derived from a simple leader model [*Bazelyan and Raizer,* 2000, p. 62] with the known potential and speed is about 3 times larger than the value found from the measured current moment with an assumption of the lower end of the leader at 13 km altitude [*Liu et al.,* 2015]. We therefore assume that the electric field in the streamer zone is smaller and that it is the critical field for positive streamers.

With this assumption, the leader tip potential and current of event 1 are estimated to be 10 MV and 35 A, respectively, when it reaches 42 km altitude. The current agrees reasonably well (about 40% larger) with the value derived from the current moment. The two quantities for the event 7 right before the final jump are 28 MV and 180 A, respectively. However, when the leaders just exit from the cloud, their potential and current could be significantly different from those values. According to the binary leader theory of lightning development [*Bazelyan and Raizer,* 2000, p. 153], a leader acquires an average potential of the thundercloud volume occupied by itself, and as the leader develops, its potential may undergo substantial changes. Assuming the lower end of the leader is at 13 km altitude, the leader current for event 1 is about 340 A and the derived potential is 100 MV, when the leader just exits from the thunderstorm. For event 7, they are 270 A and 70 MV. Surprisingly, the leader of the jet event initially has a larger current and potential than those of the gigantic jet [*Liu et al.,* 2015].

3. Sprites

3.1 Overview

In contrast to starters, jets, and gigantic jets that originate either deep inside thunderstorms or near thunderstorm tops, and propagate upward into the middle and upper atmosphere, sprites are initiated at much higher altitudes, about 70-85 km, and mainly propagate downward. They are electrical discharges triggered by sudden establishment of a strong quasi-electrostatic (QE) field above thunderclouds due to intense cloud-to-ground lightning (CG) strokes [e.g., *Pasko et al.,* 1997]. Most of sprites are caused by +CGs that produce a downward electric field above thunderstorms [e.g., *Boccippio et al.,* 1995; *Williams et al.,* 2006, 2007, 2012], and only a few per thousand observed sprites are caused by –CGs [*Barrington-Leigh et al.,* 2001; *Taylor et al.,* 2008; *Li et al.,* 2012; *Cummer et al.,* 2013].

Sprites can span an altitude range of 40-90 km above thunderstorms, with a typical lateral extent of 5-10 km [*Sentman et al.,* 1995; *Stenbaek-Nielsen et al.,* 2000; *Cummer et al.,* 2006; *Stenbaek-Nielsen and McHarg,* 2008; *Neubert et al.,* 2008; *Stenbaek-Nielsen et al.,* 2013]. Therefore, the total volume of the atmosphere affected by sprites can be as large as thousands of cubic kilometers. The luminosity of sprites typically lasts for a few to tens of milliseconds, but the electrical and chemical modifications of the atmospheric volume by sprites may last much longer [*Stenbaek-Nielsen et al.,* 2000]. In color images, they appear to be reddish above ~50 km altitude and transition to be bluish below [*Sentman et al.,* 1995]. Figure 10 shows a bright sprite recorded by a digital, low-light-level, 1000 frame per second intensified CCD imager [*Stenbaek-Nielsen et al.,* 2000]. The original black and white image is reproduced in false color to show the altitude variations of its structure and brightness [*Pasko and Stenbaek-Nielsen,* 2002]. The event shows typical morphology of sprites including a diffuse glow at the top, tendril structures at the bottom, and a distinct transition region in the middle.

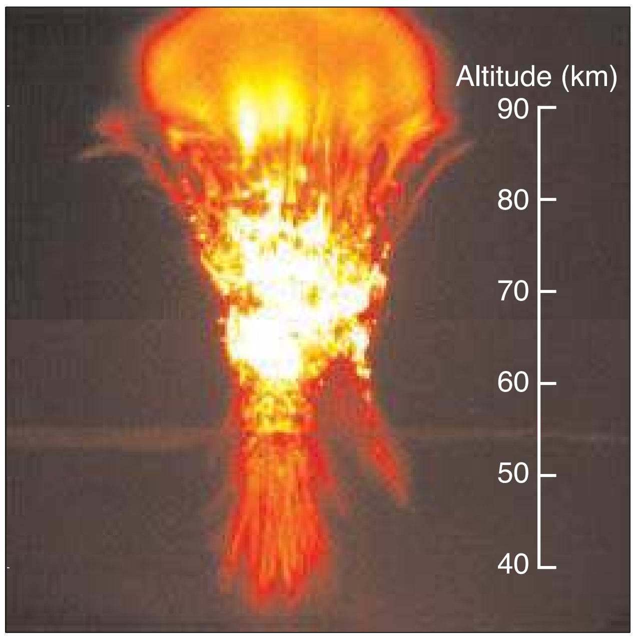

Figure 10. A large, bright sprite recorded on 18 August 1999 from the University of Wyoming Infrared Observatory [*Stenbaek-Nielsen et al.,* 2000; *Pasko and Stenbaek-Nielsen,* 2002].

Images recorded with even higher speed and/or improved spatial resolution indicate that electrical discharge processes known as streamers at atmospheric pressure are the building blocks of sprites [e.g., *Gerken et al.,* 2000; *Gerken and*

Inan, 2002, 2003; *Marshall and Inan*, 2005; *Cummer et al.,* 2006; *McHarg et al.,* 2007; *Stenbaek-Nielsen et al.,* 2007; *Stenbaek-Nielsen and McHarg,* 2008]. Streamers are nonlinear ionization waves. They create cold (typically less than 400-500 K), filamentary plasma channels as they propagate. The electric field in the streamer head or the ionization wave front is very large. Electrons are accelerated to high energies in the streamer head, and collisions between them and neutral molecules lead to ionization and excitation, resulting in luminous streamer heads.

In the figure below and sections 3.2-3.4, we show high speed images of a few sprite events. The observations were made with two intensified high-speed CMOS cameras, a 12 bit Phantom v7.1 and a 14 bit Phantom v7.3 (see [*McHarg et al.,* 2007; *Stenbaek-Nielsen et al.,* 2007; *Stenbaek-Nielsen and McHarg,* 2008; *Stenbaek-Nielsen et al.,* 2013] for a detailed description of the two imaging systems). Both cameras have 800x600 pixel detectors, but the actual image size recorded is software controlled and for most of our sprite observations we typically use a smaller size image to extend recording time. The intensifier units are VideoScope VS4-1845HS with 1 microsecond phosphors (P-24), and hence, there is no image signal carried into the following images due to intensifier phosphor persistence. The intensifier spectral responses are slightly different, but this does not affect the data and conclusions presented here.

Figure 11 shows a sprite event captured by the two high-speed imagers with different field of views. Panel (a) is a composite image obtained by averaging over 13 frames (a total duration of 1.04 ms with 78 microsecond integration time for each frame) recorded by one of the imagers with a relatively large field of view. It clearly shows tendril structures that are typically observed by an imager system with an integration time greater than 1 ms. Panel (b) shows a single frame recorded by the other high-speed imager (20 microsecond integration time) with a narrow field of view corresponding to the small rectangular area in the center of Panel (a). The bright blobs in the image are streamer heads. The tendril structures in images with longer integration time, in fact, form from continual exposure of the detector to fast moving streamer heads, and they show the paths of individual bright streamer heads. The streamer head size varies from many tens to a few hundreds of meters [e.g., *Gerken et al.,* 2000; *Gerken and Inan*, 2002, 2003; *Marshall and Inan*, 2005; *McHarg et al.,* 2007; *Stenbaek-Nielsen et al.,* 2007; *Stenbaek-Nielsen and McHarg,* 2008; *McHarg et al.,* 2010; *Kanmae et al.,* 2012]. This event is analyzed in more detail in Section 3.4 to study streamer branching dynamics, one of the actively pursued research subjects in sprites and streamers.

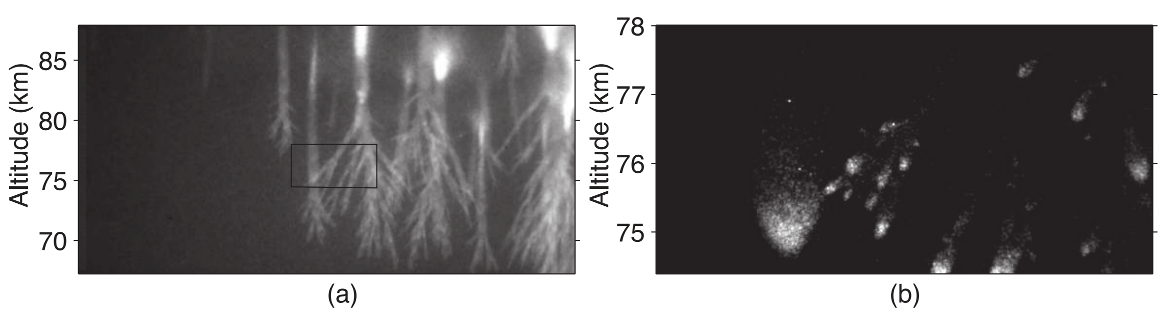

Figure 11. (a) A composite image of a sprite event recorded by a high speed imager on 15 July 2010. (b) A telescopic image of the small rectangular area in the center of (a) recorded by another high speed imager.

The occurrence of sprites above thunderclouds was predicted by the Nobel Prize Laureate C.T.R. Wilson 90 years ago [*Wilson,* 1925]. He suggested that strong electric field could appear above thunderstorms due to charge redistribution by lightning flashes or charge imbalances in thunderstorms. Under extreme circumstances, the electric field can exceed the electrical breakdown threshold field of air at high altitudes, resulting in electrical discharges or sprites. Figure 12 illustrates this idea by showing a comparison of the altitude profile of the electrical field produced by a CG stroke to the threshold field of conventional electrical breakdown E_k. Before a CG stroke, the electric field above thunderstorms is very small as a result of collective action of cloud charges, space charges induced in the conducting atmosphere, and their image charges in ground. A CG stroke quickly neutralizes a certain amount of positive or negative charge inside thunderstorms. This is equivalent to introduce the same amount of charge but opposite polarity at the same location. The simplest model to estimate the electric field produced by a CG stroke is an electric dipole consisting of the equivalent charge transferred by the lightning to the thunderstorm altitude and its image in ground. The solid line in Figure 12 shows the dipole field produced by a cloud charge of 100 C at 10 km altitude [*Pasko,* 2010, and References cited therein]. The field decreases with altitude r as r^{-3}. The conventional breakdown threshold field E_k, on the other hand, falls exponentially with increasing altitude, because it is proportional to air density that exponentially decreases with altitude (see Figure 2). Therefore, "there will be a height above which the electric force due to the cloud exceeds the sparking limit" [*Wilson,* 1925], resulting in electrical discharges above thunderstorms.

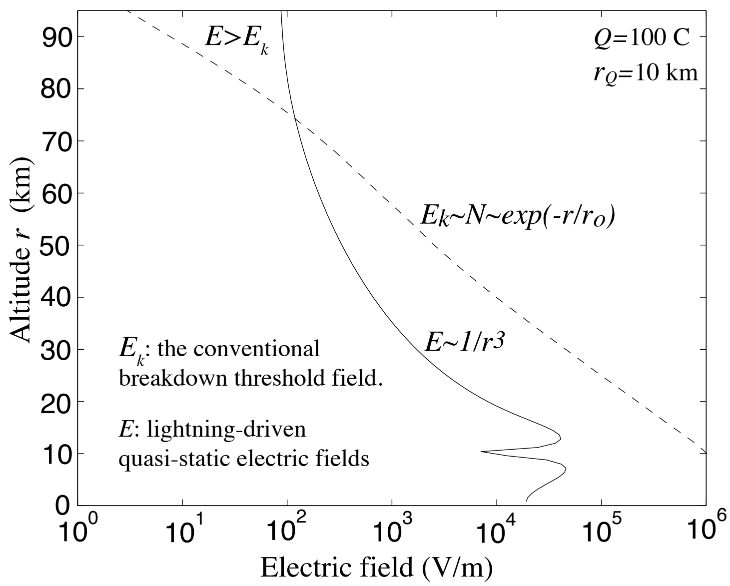

Figure 12. Physical mechanism of sprites [*Wilson,* 1925]: "While the electric force due to the thundercloud falls off rapidly as *r* increases, the electric force required to causing sparking (which for a given composition of the air is proportional to its density) falls off still more rapidly. Thus, if the electric moment of a cloud is not too small, there will be a height above which the electric force due to the cloud exceeds the sparking limit" [*Pasko,* 2010, and references cited therein].

The electric field of an electric dipole is directly proportional to its dipole moment. In the sprite literature, the charge moment change is more commonly used to measure the strength of lightning for triggering sprites [*e.g., Cummer and Inan,* 1997; *Cummer,* 2003; *Cummer et al.,* 2013]. It is the amount of charge removed by the lightning multiplied by the altitude from which it is removed, thus equal to half of the dipole moment of the electric dipole consisting of the charge removed by the lightning and its image.

The physical mechanism of sprites illustrated by Figure 12 has been tested by careful analyses integrating sprite videos, lightning current measurements, and lightning field simulations [*Cummer and Lyons*, 2005; *Hu et al.,* 2007; *Li et al.,* 2008; *Gamerota et al.,* 2011, *Li et al.,* 2012]. The results indicate that it can predict the initiation of bright, short-delayed (<~10 ms from the parent lightning return stroke) sprites reasonably well: prompt sprites are initiated when the lightning field reaches about 0.8E_k. For long delayed or dimmer sprites, those studies find that sprites can be initiated in a lightning field as low as 0.2-0.6E_k [*Hu et al.,* 2007; *Li et al.,* 2008; *Gamerota et al.,* 2011]. Recent modeling studies indicate that the initiation of sprites in the field well below E_k can be explained by initiation of streamers from ionospheric inhomogeneities, although details still need to be worked out [*Liu et al*., 2012, *Kosar et al.*, 2012, 2013]. To summarize, sprites are driven by conventional electrical discharge processes, predominately by streamers, which are caused by the establishment of a QE field in the upper atmosphere by CGs.

In the following sections, we present high-speed images of a few sprite events to illustrate the spatial and temporal properties of sprites with particular emphasis on the dynamics of sprite streamers. The characteristic spatial and temporal scales of streamers at different air densities can be estimated by using the similarity laws of gas discharge physics, which suggest they scale inversely with air density [*Pasko,* 2006; *Ebert et al.,* 2006; *Liu*, 2014]. Their values at 70 km altitude are about 15,000 times larger than at ground pressure. This makes it possible to obtain consecutive images of the same streamer by using currently available high-speed cameras, which allows for detailed investigation of the properties and physics of the streamer. It should be mentioned that many research topics in sprites that are actively investigated by various research groups are not covered here, such as sprite spectra [e.g., *Kuo et al.,* 2005; *Liu et al.*, 2006, 2009b; *Liu and Pasko,* 2007, 2010; *Mende et al.,* 2006; *Liu et al.,* 2009b; *Kanmae et al.,* 2010], radio frequency measurements [e.g., *Cummer et al.,* 1998; *Füllekrug et al.,* 2001; *Li and Cummer,* 2011; *Füllekrug et al.,* 2010, 2011; *Cummer et al.,* 2013], effects on the radio wave propagation [e.g*., Moore et al.*, 2003; *Inan et al.,* 2010; *Haldoupis et al.,* 2010, 2012], chemical effects [e.g., *Sentman et al.,* 2008; *Gordillo-Vázquez,* 2008; *Arnone et al.,* 2014], and infrasound emissions [*Liszka,* 2004; *Farges et al.,* 2005; *Farges and Blanc,* 2010; *Pasko,* 2009; *de Larquier and Pasko,* 2010; *da Silva and Pasko;* 2014].

3.2 Streamer initiation

The initiation of streamers is not well understood. Observations show they either originate out of the dark background or originate from structures within a preceding halo. In many events the halo is so bright that it saturates images, which makes it impossible to extract detailed information about the streamer initiation. Figure 13 shows an example with streamers emerging out of the dark background. The event was observed from Langmuir Observatory, New Mexico, looking east on 9 July 2005 at 04:15:17 UT. The observations were made at

10,000 frames per second. The top image is one frame 2.3 ms after the appearance of the first streamer head. As seen in the image there are multiple streamers all moving straight down. Below is an image time series to illustrate the sprite streamer initiation. The time series was made from consecutive image sections covering the dominant streamer as indicated by the box in the image at top. The altitude scale to the right is derived assuming that the sprite occurred at the range of the causal lightning strike as reported by NLDN.

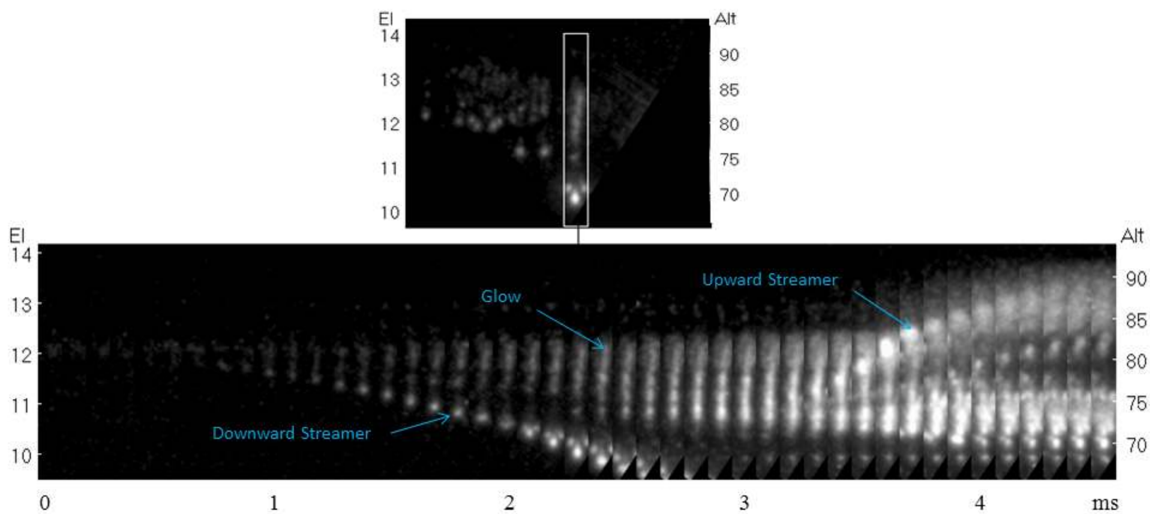

Figure 13. Streamer initiation in a bright sprite observed from Langmuir Observatory, New Mexico, on 09 July 2005 at 04:15:17 UT. The recording was made at 10,000 frames per second. The top shows one frame 2.3 ms after first streamer detection. The image time series (bottom) was created by extracting strips from 45 successive images starting with the first image in which the streamer is detected. The strip location within the full image is given by the white box. The elevation angle of the observation is shown on the left and altitude on the right. The altitude was derived assuming the sprite over the causal lightning

strike as recorded by NLDN. The sprite starts with a downward propagating streamer head, and a stationary glow gradually appears in the space around the onset altitude. The upward streamer head starts later and from a lower altitude; it also starts from existing sprite structure. The maximum downward and upward streamer head velocities are 1.3×10^7 m/s and 2.3×10^7 m/s respectively.

Figure 13 illustrates well some main characteristics of sprites. All sprites start with downward propagating streamers. In this example the onset is at an altitude of 81 km. The streamer has a bright head that propagates downward at increasing speed as indicated by the steepening track of the streamer head in the time series plot. Near the onset altitude a stationary glow gradually appears. This glow is often the main optical feature in low time resolution images (photographs or standard 30 fps video recordings). In some events also upward propagating streamers may appear. When they do, as in this example, they appear later, from a lower altitude, and from near the bottom sprite glow created by earlier downward propagating streamers.

To properly understand the observations of the streamer initiation one has to recognize that the recording imager has a finite sensitivity and that there is a minimum detectable brightness. Thus, the streamer initiation may actually take place at some earlier time with the initial optical emissions below the minimum detectable brightness [*Liu et al.*, 2009a; *Qin et al.*, 2012a]. In the study by *Liu et al.* [2009a] we found by comparing the simulations with an observed event that the optical emissions from the streamer only became detectable 0.58 ms after streamer initiation.

Many sprite events follow a visible halo within which the streamers form. Our many years of sprite observations clearly show that the brightness of the sprite halo can vary considerably between events. Recognizing this *Luque and Ebert* [2009] have suggested that sprite streamers originate from the collapse of a screening-ionization wave, which is the halo, but that in some events the halo may simply not be bright enough to be observed. Other studies indicate that the streamers originate from mesospheric irregularities [*Qin et al.,* 2011, 2012a, b, 2014; *Liu et al.,* 2012, 2014; *Kosar et al.,* 2012, 2013; *Füllekrug et al.,* 2013]. Figure 14 shows data from two events where streamers appear from visible structures in the halo. The events were recorded on the NSF supported Gulfstream V aircraft on 27 August 2009 flying at 14 km altitude over Oklahoma. Both events had elve, halo and streamers clearly visible in the images. The imager was operated at 16,000 frames per second (62.5 microseconds between images) with a field of view of 15.2x6.0 degrees.

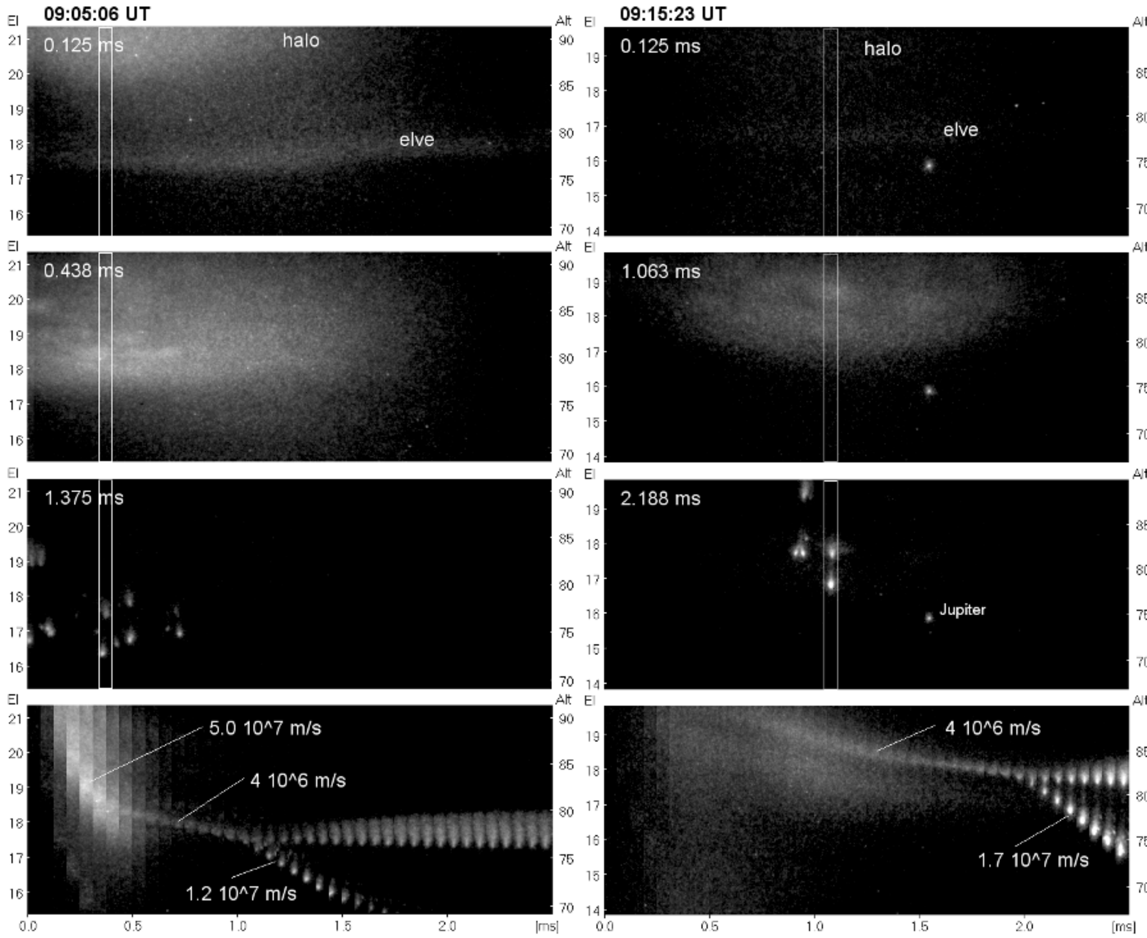

Figure 14. Two events with sprite streamers initiated from structure in the halo. The events were recorded at 16,000 fps on a Gulfstream V aircraft flying over Oklahoma on 27 August 2009 at 09:05:06 UT (left) and at 09:15:23 UT (right). The three top panels are selected high speed images showing elve, halo and streamers. The bottom panels show image time series covering 2.5 ms of time illustrating the streamer development and the downward movements of the halo and streamer. The image time series are constructed of image strips from sequential images. The location of the strip within the images is indicated by the white box. The time axis, and the time on the images, is time from the first appearance of the elve. The altitude scale was calculated assuming the sprite at

the range of the causal lightning strike as reported by NLDN. The bright point-like feature lower center right in the images from the 09:15:23 UT event is the planet Jupiter. The Gulfstream aircraft was operated by NCAR with NSF support.

In the top image the elve is seen across the center and the halo is just entering the field of view from above. The second image has the halo with clear spatial structures which later spawned streamers as evident in the third image. To illustrate the streamer development and the downward motion sub-images from 40 successive frames, corresponding to 2.5 ms total time, were extracted to form an image time series starting with the image in which the elve first appears. The image time series are shown in the bottom panel. The white box on the full images show the image region extracted in each of the two events. The altitude scale was derived assuming that the sprite was directly above the causal lightning strike as recorded by NLDN. The elve and halo in the 09:05:06 UT event are roughly 3 times brighter than in the 09:15:23 UT event, but the latter has brighter streamers. The event at 09:15:23 UT was a rather small and not particularly bright event, but even so, the brightness of the streamers is clearly brighter than the planet Jupiter, which happened to be within field of view.

The two events have visible spatial structures within the halo, and the spatial structures form the seed for streamer formation. The larger diffuse halo appears to fade prior to streamer formation, which is also observed in many events in our larger high speed imager data set. It is important to note that the observation of halo structure leading to streamer formation, while not at all infrequent, is not generally the case. A significant fraction of our sprite events has the streamers emerging from the dark background, but, as mentioned above, this could just be an artifact of the imager sensitivity. A quantitative analysis of the occurrence rate of halo structure in our large data set has not been done, but *Moudry et al.* [2003] reported that about half of 23 halos observed on 18 august 1999 from the Wyoming Infrared Observatory (WIRO) near Laramie, Wyoming, had internal spatial structure.

The time from lightning strike to sprite streamer initiation varies considerably in our observations as does the altitude of streamer onset. In the two events shown in Figure 14 individual streamers appear over a 6 ms interval from the first detection of the elve that is created by the electro-magnetic pulse radiated from the lightning strike. The appearance of the elve is often used to time events. The two events are relatively small sprites. In larger events we typically see many streamers form. An example is shown in Figure 15 (top). Here more than 20 streamers are initiated within 1.2 ms of the appearance of the elve. In other events streamer formation only occurs later. In the example shown in Figure 15 (bottom) the streamer onset is at 12.9 ms. These two events were observed from two aircraft flying over Iowa and Nebraska, respectively. The altitude scales given are based on triangulation. There are observations of sprites with streamer onset as late as almost 100 ms after the strike [*Li et al.,* 2008; *Gamerota et al.*, 2011]. The reason for delayed streamer formation is uncertain. *Li et al.,* [2008] have suggested that the continuing current, as originally proposed by *Cummer and Füllekrug* [2001], plays an important role. *Luque and Gordillo-Vázquez* [2012] have proposed electron detachment from O^-

ions can cause the delay. On the basis of detailed modeling results, *Liu et al.* [2014] have suggested that the delay is the result of streamer initiation from gradually-amplifying mesospheric inhomogeneities near a halo front that may be invisible. In this case, the inhomogeneities can be small-scale, weak-amplitude perturbations created by atmospheric processes such as gravity waves. The amplification can take place in an electric field below the conventional breakdown field because of the electron detachment process from O^- ions [*Luque and Gordillo-Vázquez,* 2012; *Liu,* 2012; *Neubert and Chanrion*, 2013] but requires a longer time, which contributes to the delay of the streamer initiation.

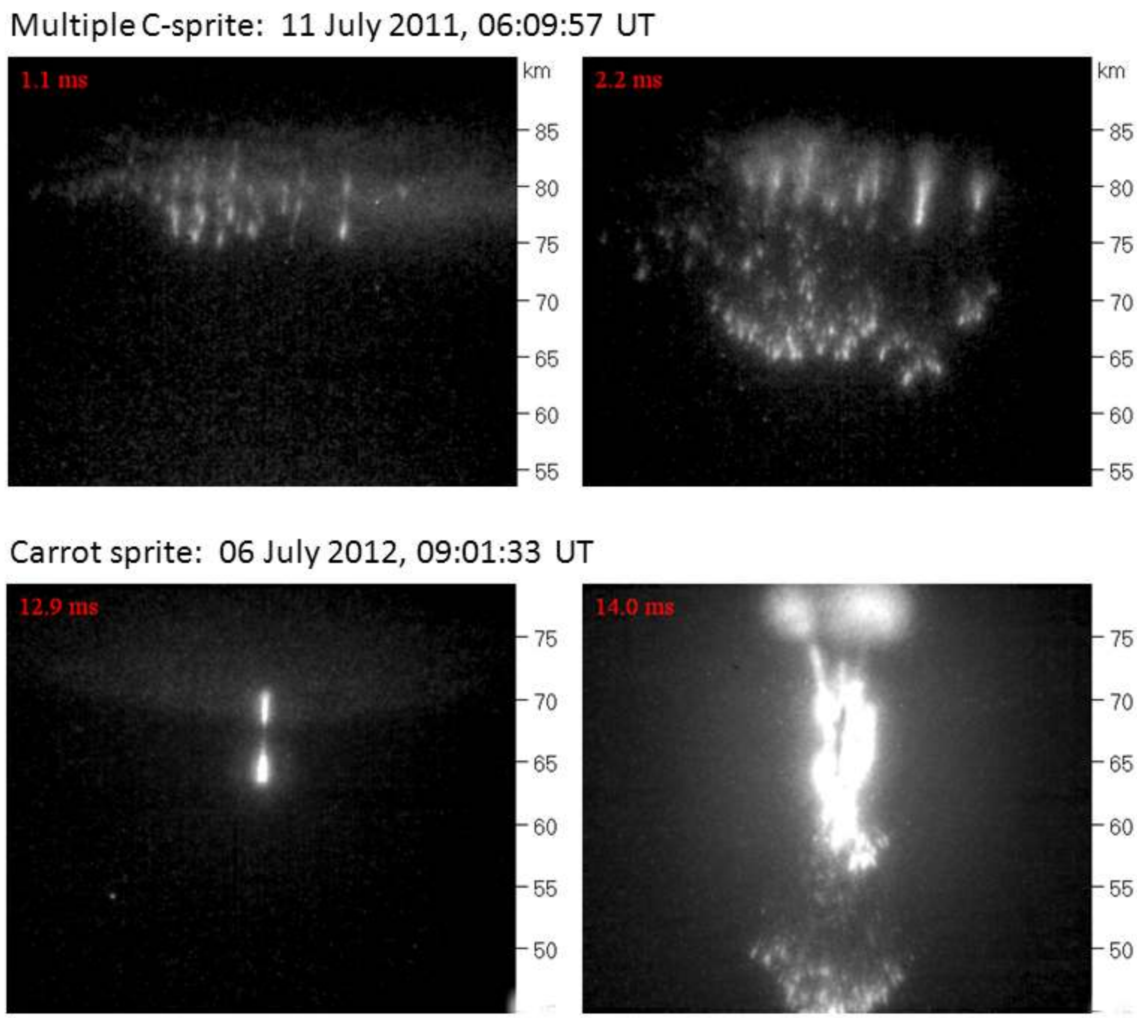

Figure 15. Top: Multiple C-sprite event observed from aircraft over Iowa on 11 July 2011 at 06:09:57 UT. Numerous streamers were launched from the halo within 1 ms of the appearance of the elve. Bottom: Carrot sprite observed over Nebraska on 6 July 2011 at 09:01:33 UT. The initial streamer did not appear before 12 ms after the elve. Both events were recorded at 10,000 fps. Observations were made from 2 aircraft flying 30 km apart so the location and altitude of the sprites could be triangulated. The 2011 sprite campaign was sponsored by the Japanese Broadcasting Corporation (NHK).

The altitude of streamer initiation varies as well. Triangulated onset altitudes from 66 km to 89 km for downward propagating streamers and 64 km to 78 km for upward propagating streamers have been published by *Stenbaek-Nielsen et al.* [2010]. Higher altitude streamer initiation is typically associated with C-sprites. Sprites with streamer onset in the few millisecond range are categorized as prompt sprites, and they are expected to have their onset at relatively high altitude, 80 km or higher [*Hu et al.*, 2007; *Li et al.*, 2008], whereas delayed sprites have their onset at lower altitudes, which has been verified through triangulation [*Gamerota et al.*, 2011].

The propagating streamers define the type of sprites. With only downward streamers the sprite would be characterized as a C-sprite or multiple C-sprites (Figure 15 top), while, if there are upward propagating streamers, the sprite would likely be characterized as a carrot sprite (Figure 15 bottom). It must be noted that the number of upward streamers vary greatly between events and the classification of a given sprite event as either C-sprites or carrot sprites is often subjective [*Stenbaek-Nielsen et al.,* 2008]. It should also be noted that prompt sprites are typically multiple C-sprites while delayed sprites tend to be carrots.

Sprite streamers are high-altitude analogs of streamers discharges observed for spark or lightning discharges [*Pasko et al.,* 1998; *Liu and Pasko,* 2004; Pasko, 2006, 2007; *Ebert et al.,* 2006; *Liu*, 2014]. They have been modeled by several groups [*Liu and Pasko*, 2004; *Ebert et al*., 2006; *Chanrion and Neubert*, 2008; *Liu et al.*, 2009a, b; *Luque and Ebert*, 2009; *Liu,* 2010; *Luque and Ebert,* 2010; *Luque and Gordillo-Vázquez,* 2011; *Qin et al.,* 2012a, 2012b, 2013; *Liu et al.,* 2012; *Kosar et al.,* 2012, 2013]. As noted above the cause for streamer initiation is uncertain, and in most models the streamer development is initiated by an artificially introduced electron density perturbation that serves as a seed for the streamer. In the mesosphere perturbations of neutral or electron density may be common as they can result from effects of atmospheric waves, dust, or metallic ion layers. *Wescott et al.* [2001b] and *Zabotin et al.* [2001] suggested an association with meteors and meteor dust. *Füllekrug et al.* [2013] have presented observations of streamer initiation from an existing mesospheric irregularity. Modeling studies assuming mesospheric irregularities have been done by *Qin et al.* [2012a, 2012b, 2013, 2014], *Liu et al.* [2012, 2014], and *Kosar et al.* [2012, 2013].

It should be mentioned that modeling studies [e.g., *Liu and Pasko*, 2004; *Qin et al.*, 2012] have suggested that when an electric field greater than the breakdown field E_k is suddenly established in the lower ionosphere, sprites can be initiated from development of double-headed streamers seeded by strong inhomogeneities. In such an event two streamers of opposite polarity originate simultaneously from the same point propagating up and down. However, we have never identified such events in our substantial data set recorded over nearly 15 years. According to *Qin et al.* [2011] and *Sun et al.* [2013], when the inhomogeneities are relatively weak or no inhomogeneities exist in the lower ionosphere, only a halo will result.

3.3 Streamer propagation characteristics

Sprite streamers appear to propagate in the direction of the local electric field. The direction of the first streamers is typically straight down as seen in Figure 15 above. The onset location may not be directly above the causal lightning strike, but several tens of km away [*Lyons et al.,* 1996; *Wescott et al.,* 2001b], and in those cases the lower altitude section of the streamer paths may bend towards the location of the causal strike [*Stenbaek-Nielsen et al.,* 2000], or more accurately, towards the location of the charge removed by the lightning. Streamers forming later, notably upward propagating streamers, typically have large horizontal velocity components, which accounts for the broad tops observed in carrot sprites.

High speed observations of streamers formed after the initial bursts of downward streamers often find them propagating towards and connecting with earlier formed streamer channels and beads [*Cummer et al.*, 2006, *Stenbaek-Nielsen and McHarg*, 2008; *Montanya et al.,* 2009; *Stenbaek-Nielsen et al.,* 2013]. This is also observed in laboratory discharges [*Nijdam et al.,* 2009]. A triangulated example presented by *Stenbaek-Nielsen et al.,* [2013] (their Figure 7) shows the streamer head to connect at right angles to the streamer channel. This indicates that the channel has high conductivity consistent with the concept of streamers as ionization waves. *Gordillo-Vázquez and Luque* [2010] find the high conductivity channel to last several minutes thus providing a possible explanation for the often observed ‘re-ignition’ of sprite structures. In such events subsequent lightning activity will cause old sprite structures to re-appear even after the initial optical emissions have subsided [*Stenbaek-Nielsen et al.,* 2000; *Sentman et al.,* 2008].

Sprite streamer velocities are typically in the 10^6 to 10^8 m/s range [*Stanley et al.*, 1999; *Moudry et al.*, 2002; *McHarg et al.*, 2002; *Cummer et al.*, 2006; *McHarg et al.*, 2007; *Stenbaek-Nielsen and McHarg*, 2008]. The fastest streamer we have observed in our high speed data is 1.4×10^8 m/s, half the speed of light, inferred from multi-anode photometer observations [*McHarg et al.,* 2002]. The velocity range of downward and upward propagating streamers is very similar, but with the upward streamers typically slightly faster. The velocity of 1.4×10^8 m/s was in an upward propagating streamer. In sprite observations streamers typically propagate to the lowest altitude near the center axis of the event, and these streamers are also the fastest [*Li and Cummer*, 2009].

In image time-series plots, such as in Figures 13 and 14 above, the streamer velocity can be inferred from the slope of the streamer path. The maximum velocity for the downward streamers shown in Figures 13 and 14 are 1.3×10^7, 1.2×10^7, and 1.7×10^7 m/s respectively, and for the upward streamer in Figure 13 2.3×10^7 m/s.

The sprite halo generally descends with a velocity around 10^6 m/s. This is also seen in simulations [e.g., *Liu*, 2012]. The halo in the 09:15:23 UT event (Figure 14, left) initially has a velocity in the same range as streamers, but slows down to near 10^6 m/s prior to streamer formation. Figure 16 shows the distribution of streamer head altitudes as function of time for the multiple C-sprite event shown in Figure 15 (top). The event was observed from two aircraft flying about 30 km apart and streamer head locations were determined by triangulation. The plot has nearly 1200 triangulated positions from more than 30 individual streamers. For this event the streamer velocities vary between $3.2\text{x}10^6$ and $1.5\text{x}10^7$ m/s.

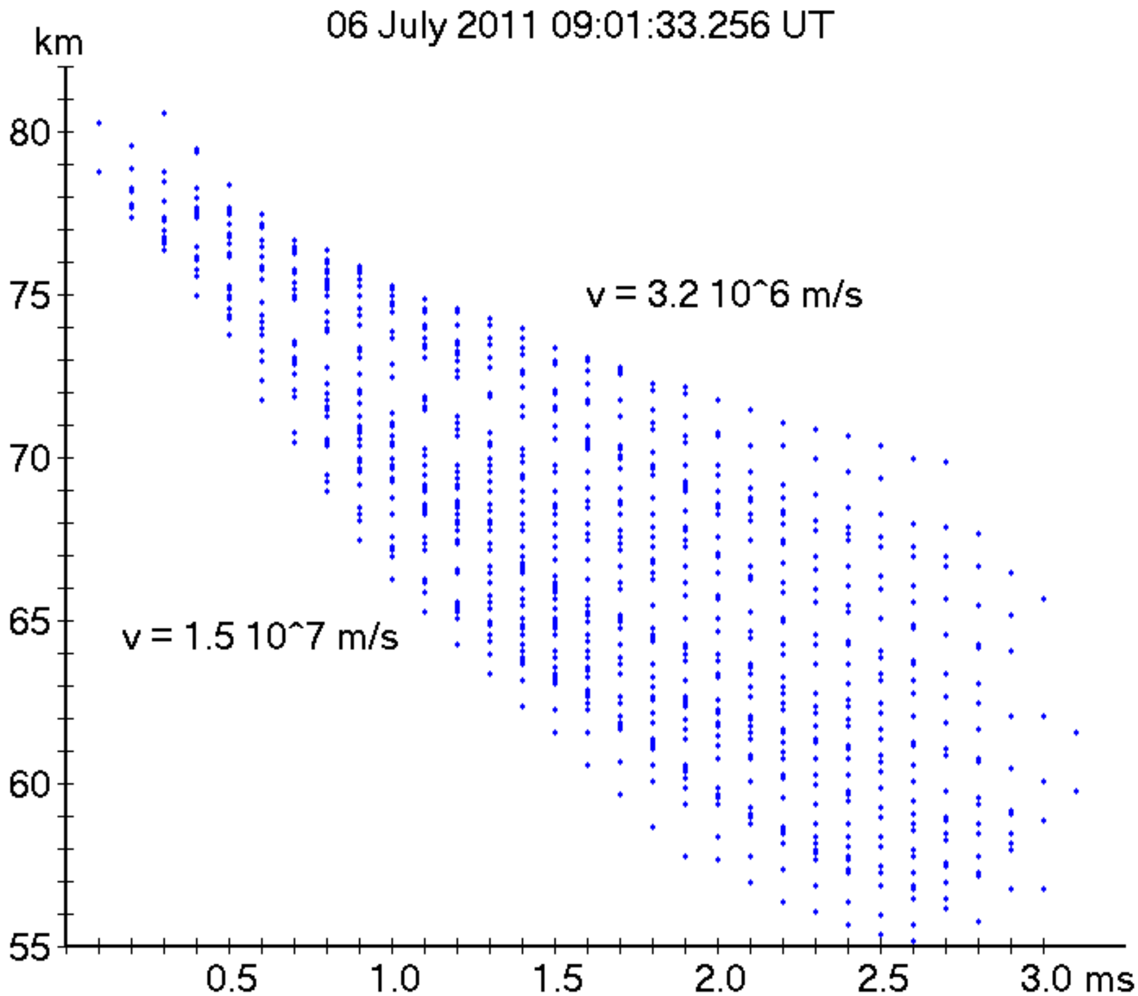

Figure 16. Altitude versus time for nearly 1200 triangulated streamer head positions. The event was recorded at 10,000 fps on 11 July 2011 at 06:09:57 UT from 2 aircraft flying 30 km apart over Iowa. 2 frames from the event were presented earlier in Figure 15 showing the numerous downward propagating

streamers. There are many splittings in the streamers and around 2 ms in the figure more than 30 individual streamers were followed. The streamers are mainly going straight down so the velocities can be calculated from the slope of their path in the plot. The flights were part of a sprite campaign funded by the Japanese Broadcasting Corporation (NHK).

The streamers initially accelerate to their maximum speed and then gradually slow down and fade. In Figure 16 the initial streamer acceleration is not obvious in the plot, but the deceleration towards the end is clear. The acceleration observed in this and other examples is generally in the 10^5-10^{10} m/s/s range [*McHarg et al.,* 2007; *Li and Cummer,* 2009]. *Li and Cummer* [2009] note that the deceleration is nearly constant, 10^{10} m/s/s, across most sprites. For the analysis leading to Figure 16 we did not relate streamer location relative to the central axis for the event where, as noted by *Li and Cummer* [2009], we should expect the largest velocities, but since the data are triangulated such an analysis could be done. The streamers terminate when the local electric field driving the streamers fall below 0.05 of the local breakdown electric field, E_k [*Li and Cummer,* 2009]. With the termination field strength fixed this suggests that the streamer termination location can be used to map the spatial structure of the electric field.

Upward propagating streamers typically terminate with a luminous puff in contrast to the downward streamers that just fade. Examples of such puffs are seen at the top of the carrot sprite shown in Figure 15 (bottom). In Figure 10 the large diffuse top of the sprite is from numerous such puffs. *Pasko and Stenbaek-*

Nielsen [2002] speculated that the puff may be related to the altitude where the electric conductivity becomes too large to support streamer propagation.

The sprite streamer heads are very bright. But despite this it has actually been very difficult to assess their brightness from image data. The high velocity of the streamers will ‘smear’ the image across many pixels during exposure [*Liu et al.,* 2009a], and even so the streamers will typically saturate the image [*Stenbaek-Nielsen et al.,* 2007]. In addition, atmospheric effects together with camera optics will slightly distort the image making it appear larger than it actually is. The same effect is seen with stars, which all are point sources, but in images bright stars appear larger than dim stars. Additionally, the spatial resolution in most sprite images is insufficient to show details within the streamer head. On a positive note, the sprite simulations today are, in general, very good, and we have found the optical emissions derived from the simulations to be consistent with our observations [*Liu et al.,* 2009a]. An outline of our efforts over the last 20 years to estimate the sprite streamer brightness and relate these estimates to simulation results has been given by *Stenbaek-Nielsen et al.* [2013].

A more qualitative estimate of the sprite streamer brightness is suggested looking at the sprite presented in Figure 14 (right). This is a rather small and not particularly bright sprite, and yet, the streamers are clearly brighter than the image of planet Jupiter, which happened to be within the field of view. The signal from a bright sprite could easily be a factor of 10 brighter. This suggests that the imager should be able to detect sprites in full daylight if sprites do happen in daylight as well.

Computer simulations of sprite streamers show the optical emissions from the streamer head to come from a ‘saucer’-shaped region at the front of the streamer [*Liu and Pasko*, 2004; *Liu et al.*, 2009a, b; *Luque and Ebert*, 2009, 2010; *Qin et al.,* 2012a, 2012b, 2013; *Kosar et al.,* 2012, 2013]. Our high-speed observations do not typically have enough spatial and temporal resolution for detailed comparison. However, we do have a few observations that allow some comparison. In Figure 17, top, we show simulations published by *Luque and Ebert* [2010]. This simulation used their ‘ionization wave’ model for streamer formation [*Luque and Ebert*, 2009] with a 200-m-large initial seed. The emissions are integrated over 50 microseconds and the downward velocity is about $7x10^6$ m/s. The saucer shaped streamer head is clearly identifiable. In Figure 17, middle, we show a streamer head extracted from a recording made at 16,000 fps with 20 microsecond exposures on 15 July 2010 at 07:06:09 UT from Langmuir Laboratory, New Mexico. This is the same event shown in Figure 11, which is also discussed in more detail in the next section. The downward velocity is $2x10^7$ m/s. During the 20 microsecond exposure the streamer will move 400 m. The apparent length of the streamer in the images is roughly 600 m, so the actual length is closer to 200 m. Thus, the shape of the streamer head is more ‘saucer’-like with a width of 600 m and a thickness of 200 m. The simulated streamer head, with a similar correction for movement during ‘exposure’, is estimated at 500x200 m, very similar to the observed. This streamer is unusually large. A similar analysis by *McHarg et al.* [2010] on a larger data set finds generally smaller widths and thicknesses. Other streamer simulations have significantly smaller streamers as well, but the shape of the optical emissions from the streamer head is the same. Finally, in Figure 17, bottom, we show a laboratory streamer observation by *Nudnova and Starikovskii* [2008]. The similarity to sprite streamers is quite striking.

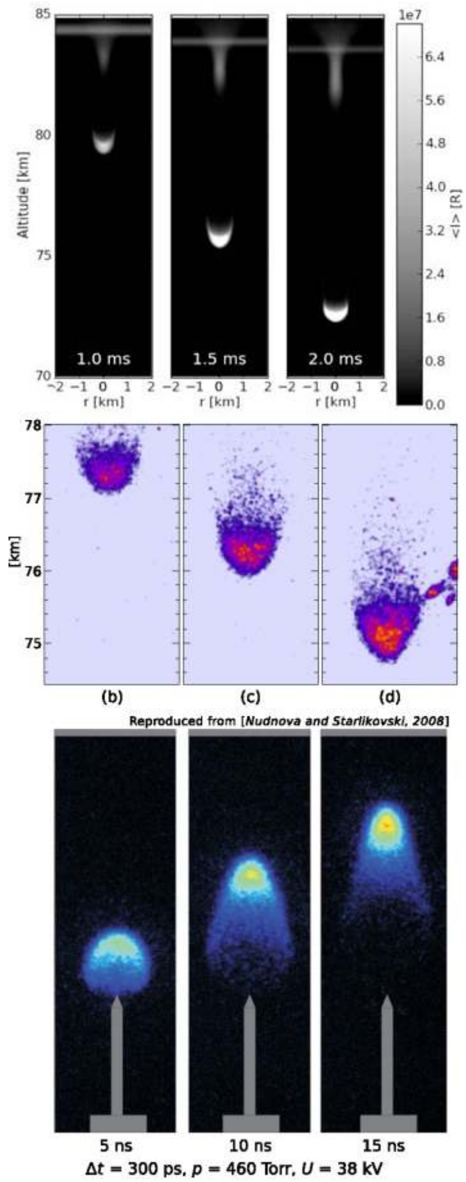

Figure 17. Simulation and observations of the saucer shaped streamer head. Top panel shows optical emissions in the streamer head reproduced from a

streamer simulation by *Luque and Ebert* [2010]. The optical emissions are from the first positive band of molecular nitrogen responsible for the large majority of the sprite optical emissions [*Kanmae et al.,* 2007]. The emissions in the simulation are integrated in space along a line of sight perpendicular to the streamer propagation and in time over 50 microseconds. Middle panel shows three successive images with a large sprite streamer recorded at 16,000 fps from Langmuir Laboratory, NM, on July 15, 2010 at 07:06:09 UT. The width of the streamer head assuming that the sprite is over the causal lightning strike as reported by NLDN is about 500 m. Bottom panel shows laboratory observations by *Nudnova and Starikovskii* [2008] of a positive streamer in a 3 cm gap with an applied voltage of 38 kV. The images are 5 ns apart and the diameter of the streamer is 4–6 mm. The observations were in air at a pressure of 460 Torr. The sprite streamer and the laboratory streamer have a remarkable similar appearance. The laboratory images were reproduced from *Nudnova and Starikovskii* [2008].

3.4 Streamer head branching

Sprite streamers are of interest to the broader discharge physics community because they serve as a natural laboratory for the study of streamer dynamics. The spatial sizes and temporal lifetimes of streamers scale with neutral density (N) as roughly 1/N [*Pasko*, 2006; *Liu*, 2014]. Thus scale sizes of sprite streamers are approximately 100 m, and lifetimes are a few tenths of milliseconds or longer. A frame rate of 10,000 frames per second (fps) can then record several frames of the same streamer tip as it propagates, allowing study of the dynamics of streamer splitting.

Previous work by *McHarg et al.* [2010] have shown that sprite streamers that propagate without splitting are less bright and smaller in width compared with splitting sprite streamers. A study of 117 streamer tips reveal the median streamer tip radius for non-splitting streamers is 193 m, while the median radius for splitting streamer tips is 389 m. Additionally, *McHarg et al.* [2010] showed a single event where an individual streamer brightened by a factor of 2.6 at the same time the radius increased from 199 to 279 m in the 300 microseconds immediately prior to splitting.

A good example demonstrating sprite streamer splitting was recorded from Langmuir Laboratory near Socorro New Mexico on 15 July 2010. In this recording we configured the two Phantom imagers with smaller fields of view, 7.3x3.7 degrees (Camera 1) and 1.3x0.6 degrees (Camera 2), to provide sprite images with better spatial resolution. Figure 18 shows the event as recorded by a Watec scene video camera with the field of views of the two high speed imagers inserted. The field of view of the Watec camera is 14.2x10.4 degrees.

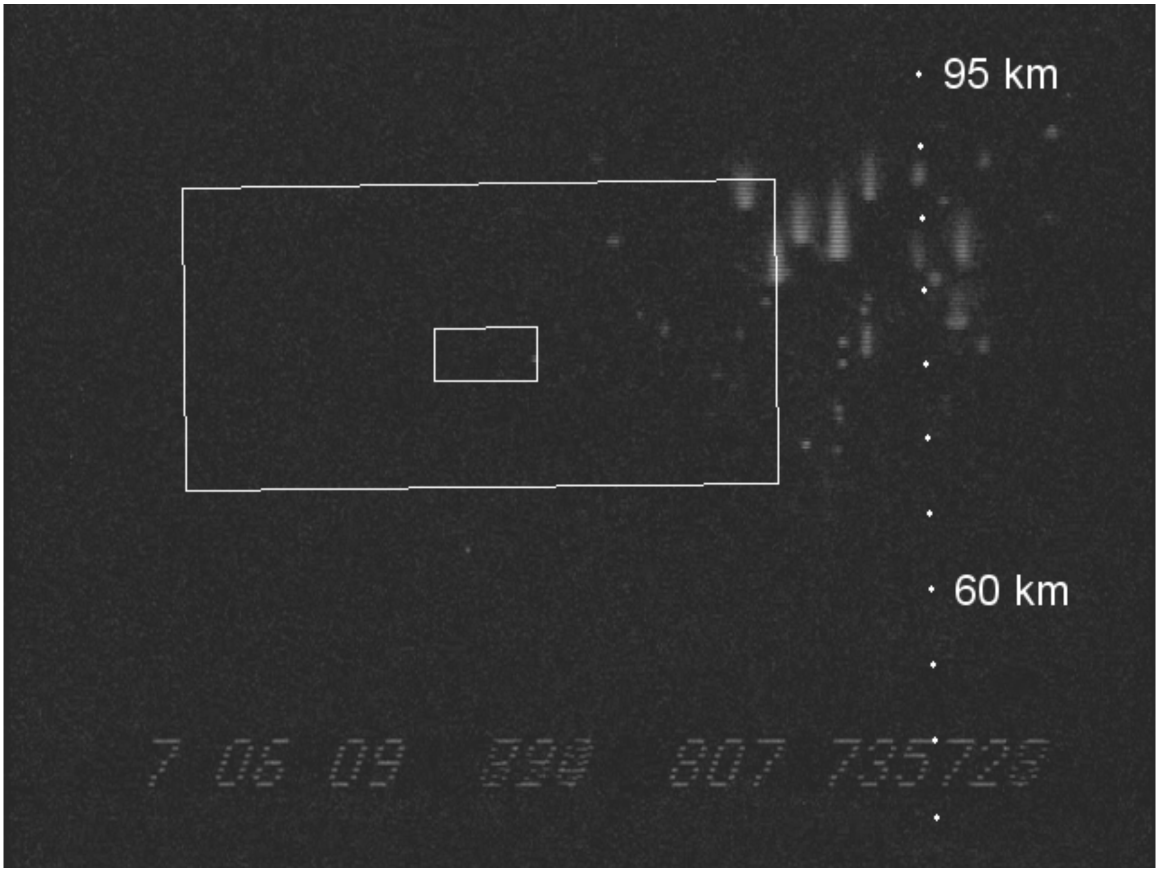

Figure 18. Video image of a multiple C-sprite event observed on 15 July 2010 at 07:06:09 UT. The field of view of the image is 14x10 degrees. Inserted are the 7.3x3.7 (Camera 1) and 1.3x0.6 (Camera 2) degree field of view of the two high-speed cameras. Points are at 5 km altitude increments above the NLDN strike.

This event would be classified as multiple C-sprites, and it is the same event shown in Figure 11 and in the middle panel of Figure 17. It is a very short duration sprite. The sprite is present in one video frame only, and in the high speed images it lasts less than 10 ms. Most of the C-sprites are outside the view of the high speed imagers, and one might expect little activity in the high speed data, but elve, halo, and streamers were all observed by both high-speed cameras. The lack of corresponding obvious sprite features in the video frame is due to the very short duration of the event combined with the high velocity downward motion of individual sprite features.

The 7.3x3.7 degree field of view of Camera 1 was recorded at 12,500 fps (80 microseconds between frames) with an integration time of 78 microseconds (2 microseconds readout time). Each image is 512x256 pixels. Figure 19 shows an average of 13 frames (1.04 ms) from camera 1. The altitude scale on the left was derived assuming the sprite to be at the same range, 310 km, as the causal lightning strike reported by NLDN. The box inside the image denotes the 1.3x0.6 degree field of view of Camera 2. This integrated image clearly shows the "tracks" of the streamer tips as they undergo splitting within the field of view. Comparison with the Watec image of Figure 18 demonstrates that the high speed camera is much more sensitive to the short duration sprite streamer dynamics.

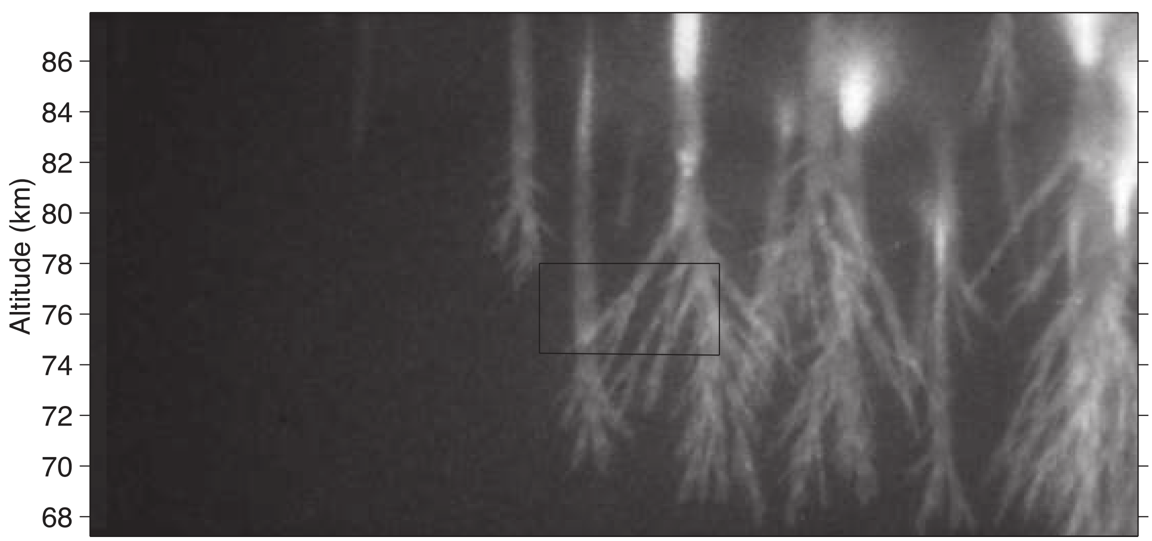

Figure 19. Average of 13 frames (1.04 ms) from Camera 1 for the sprite event observed on 15 July 2010 at 07:06:09 UT. The field of view is 7.3x3.7 degrees. This is the same image used for panel (a) in Figure 11.

Figure 20 shows six consecutive high speed images from Camera 1 in its top three rows. Again, the altitude scale on the right of each panel was derived assuming the sprite to be at the same range, 310 km, as the causal lightning strike reported by NLDN. The onset altitude indicated by the scale appears to be high. As mentioned in section 3.3 the onset location may not be directly above the causal lightning strike, but several tens of km away [*Lyons et al.,* 1996; *Wescott et al.,* 2001b]. If the sprite appears closer to the observer the elevation angle would be higher and we would infer a higher altitude. For example, if the sprite were 25 km closer the altitude scale would be 6 km too high.

The annotation in the upper left of each image is the time from the first appearance of the elve, which propagated down through the field of view in 3 or maybe 4 frames. The selected images start with the appearance of well defined halo structures moving down into the camera field of view. The horizontal width of the structures is about 5 km assuming the 310 km range. The halo structures sharpen into V shapes and a streamer head emerges from its tip. There are several such examples of streamer formation in the 6 images. The apparent width of the streamers is 1-2 km, but since most are saturated this would be an overestimate. The two streamers within the rectangular box in the right side of the images form without saturating the detector, and their widths are 0.8 km again assuming a 310 km range. The time of streamer formation within this field of view is 0.6 to 1.1 ms after the casual lightning strike. At the bottom right of the figure is an image time series formed by the image sections within the rectangular box shown from 15 consecutive frames, including the 6 images at the top of the figure. The image time series illustrate the downward propagation of both halo structures and streamers with the slope providing the velocity. As shown on the figure the downward velocity of the halo structure is 1.1×10^7 m/s and velocity of the streamer is 2.1×10^7 m/s. The full image at bottom left is the last used for the time series showing the spectacular streamer splitting occurring in this event. Comparison with the average image in Figure 19 again demonstrates that streamer tip motion is “smeared” over longer integration times.

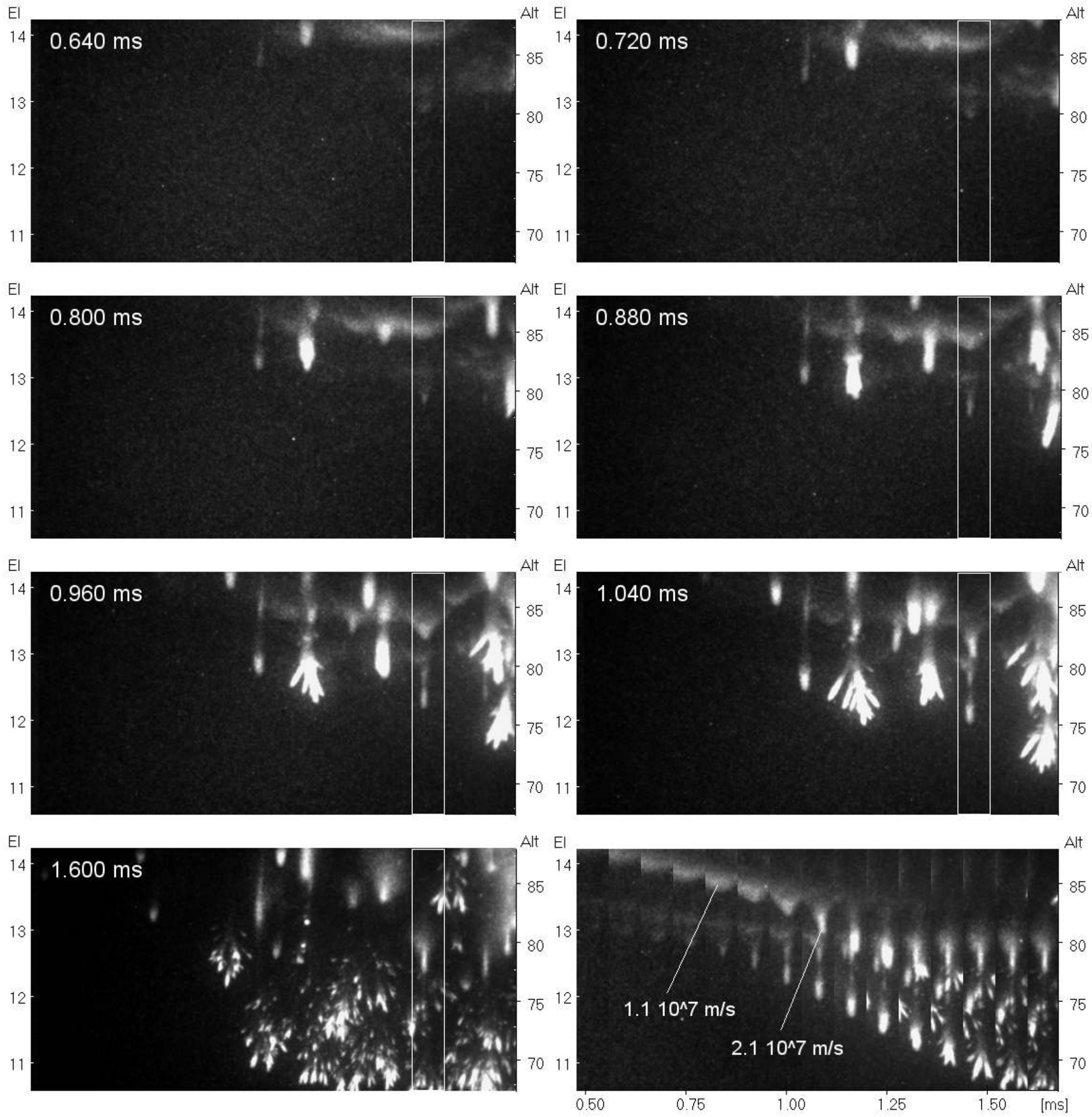

Figure 20. Images from event observed on 15 July 2010 at 07:06:09 UT recorded at a frame rate of 12,500 frames per second. The field of view is 7.3x3.7 degrees. Bottom left is the last frame used for the image time series shown in the bottom right. The image time series illustrate the streamer formation and the associated downward velocities. The times indicated are from the first appearance of the elve.

McHarg et al. [2010] shows a streamer tip with velocity $1.8x10^7$ m/s which propagates 920 m in 50 microseconds (the image integration time). The measured length of the streamer was approximately 890 m (but this number is dependent on how far down the intensity profile one goes to measure the length), and a width of 180 m. This is consistent with a streamer tip shaped like a pancake (see also Section 3.3) with a depth less than or equal to the pixel resolution, in that case 30 m, and 180 m wide.

The narrow field Camera 2 recorded data at 16,000 fps, 62.5 microseconds between images, with an integration time of 20 microseconds. Four successive images from Camera 2 are displayed in Figure 21. A false color scale is used to enhance the contrast. The annotation in the upper left of each image is the time from the first appearance of the elve, similar to Figure 20. A large streamer tip is seen to the left of each image which propagates vertically through the field of view. Figure 20 shows that this streamer splits immediately after it leaves the field of view of Camera 2. A second streamer is seen immediately to the right of the large streamer. In the successive four images it propagates down and to the left, splitting in the second image. Close inspection of the second and third image shows the streamer splitting into at least 6-10 pieces. At this frame rate, and with the 20 microseconds integration time, it is not possible to say if the streamer truly falls into 6-10 pieces from one, or if it splits repeatedly in the time between the frames. However, it is clear that sprite streamers can divide into 6-10 sub-streamers within approximately 60 microseconds.

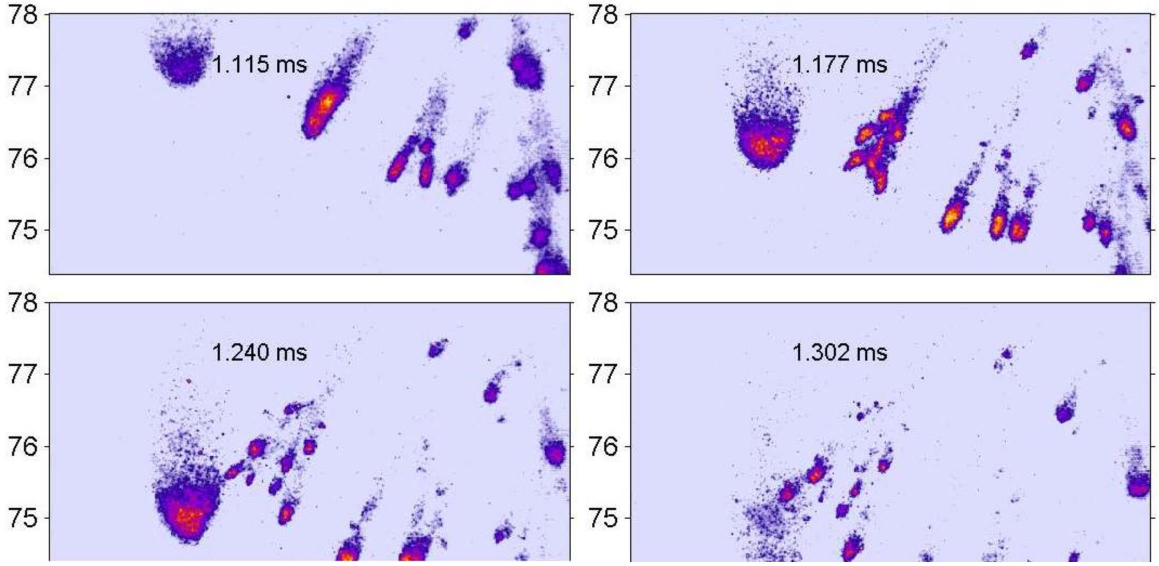

Figure 21. Images of the event observed on 15 July 2010 at 07:06:09 UT recorded at a frame rate of 16,000 frames per second. The field of view is 1.3x0.6 degrees. The annotation in the upper left is the time from the first appearance of the elve. The image pixel values are false colored to enhance the contrast of the splitting streamers.

Laboratory studies of streamers reveal that most streamers split into two branches [*Heijmans et al.,* 2013]. *Heijmans et al.* [2013] studied discharges in 100 mbar (approximately 17 km altitude in the atmosphere) artificial air exposed to 10 kV voltages pulses across a needle electrode 160mm above a grounded plate. The same study reported that approximately every 200 events in the lab results in a splitting into three branches. Using the standard atmosphere, the ratio of the density between 75 km and 17 km (100 mb) is approximately 3000. It is interesting to note that *Heijmans et al.* [2013] report streamer widths of a few mm at 100 mbar pressure. Scaled up by 3000 would be 15 m, and we observe sprite streamers with scale sizes of tens to hundreds of meters. *Heijmans et al* note that the surface area of the streamers before and after branching is about the same. This means that the branched streamer radii are less than the original streamer. This is very similar to what we observe in sprite streamers, as shown by Figure 21.

Streamer branching is poorly understood at present. Current theory suggests it is a deterministic process, but statistical factors do play a role [e.g., *Arrayas et al.,* 2002; *Rocco et al*., 2002; *Liu and Pasko*, 2004; *Ebert et al.,* 2006; *Luque and Ebert,* 2011; *Savel'eva et al.,* 2013; *Sadighi et al.,* 2015]. In general, splitting in streamer heads occurs when they grow in size and their fronts flatten. Accompanying this change in the streamer head geometry, the streamer approaches an ''ideal conductivity'' state with approximately equipotential streamer head and thus, a thin space charge layer forms on the streamer head [e.g., *Arrayas et al.,* 2002; *Rocco et al*., 2002; *Liu and Pasko*, 2004; *Ebert et al.,* 2006]. This state is dynamically unstable and leads to a Laplacian instability resulting in the streamer splitting [e.g., *Arrayas et al.,* 2002; *Rocco et al*., 2002; *Ebert et al.,* 2006]. According to the theory of the instability of a planar discharge wave front [*Ebert et al.*, 1997; *Kyuregyan*, 2012], the planar front is unstable when it is subject to transverse perturbations with spatial scales on the order of the thickness of the front (the thickness of the space charge layer). The streamer head approaching the ideal conductivity condition can be roughly approximated as a planar wave front, and perturbations with a spatial scale smaller than its width can grow faster than streamer development, leading to branching. *Liu and*

Pasko [2004] suggest that the photoionization range is an important length scale defining the maximum streamer radius and predict the value of this radius for sprite streamers. *McHarg et al.* [2010] show that the theoretical radius of 97 m for stability at altitude of 70 km is close to the observed median radius of 197 m. *Luque and Ebert* [2011] investigate possible perturbations that can give rise to streamer branching, and point out that the ratio of the distance between branching events and the streamer radius is an important parameter to measure. Laboratory measurements show this ratio to be 12-15 [*Briels et al.*, 2008, *Nijdam et al.*, 2008]. *Luque and Ebert* [2011] theoretically predict this ratio in the lab to be approximately 8, and note that it may be longer for sprite streamers, due to the reduced electron density perturbations at mesospheric altitudes. *Savel'eva et al.* [2013] and *Sadighi et al.* [2015] perform analysis of the curvature of the streamer head surface from simulations and suggest that streamer branching can naturally occur, because the flattening of the streamer head gradually moves the maximum field in the streamer head off from its symmetry axis. Nearly all the streamer simulations that have been reported are conducted by using a 2D model (3D with cylindrical symmetry), future work by using a fully 3D model is required to further our understanding of streamer branching, for example, to understand how streamer branching breaks cylindrical symmetry and how different pieces result from a single branching event.

4. Concluding remarks

This paper gives an introduction to transient luminous events. It focuses on recent ground-based video and high-speed observations of transient luminous events to illustrate their main temporal and spatial features. The theories of transient luminous events are also briefly discussed in order to provide a basic picture of our understanding of those interesting phenomena. Significant progress in understanding various aspects of transient luminous events has been made recently through coordinated and dedicated observational efforts such as satellite missions, aircraft campaigns, ground-based monitoring network, and focused theoretical and simulation studies by using electromagnetic, fluid, particle, hybrid, or fractal modeling approaches and techniques. The work in transient luminous events has benefited tremendously from the studies of electrical discharges at ground or near-ground pressure. On the other hand, the research in transient luminous events has also contributed useful knowledge to advancing our understanding of basic electrical discharge processes in air. In particular, transient luminous events provide a natural experiment to study the electrical discharge processes at low pressure that is impossible to conduct in the laboratory. The research work not only directly gives the properties of the discharges at low pressure, but also gives insight into the scaling laws of the discharges at different pressure and into the conditions of violation of the scaling laws. It also manifests the relative roles of elementary discharge processes in electrical discharges. The community of transient luminous events has traditionally been very open to interactions with researchers from other communities, and it, in fact, consists of investigators from different backgrounds and disciplines. We expect that future progress in this field will come from active interactions between our community with other communities, and from close collaborations between experimentalists, observers, modelers, and theoreticians.

Acknowledgments

This research was supported in part by NSF grants AGS-0955379 and AGS-1348046 to Florida Institute of Technology, and NSF grant AGS-1104441 to University of Alaska Fairbanks.

References

E. Arnone, A. K. Smith, C.-F. Enell, A. Kero, and B. M. Dinelli (2014), WACCM climate chemistry sensitivity to sprite perturbations, *J. Geophys. Res. Atmos.,* 119, 6958–6970, doi:10.1002/2013JD020825.

M. Arrayas, U. Ebert, and W. Hundsdorfer (2002), Spontaneous branching of anode-directed streamers between planar electrodes, *Phys. Rev. Lett.*, 88, 174502(R), doi:10.1103/PhysRevLett.88.174502.

E. M. Bazelyan and Y. P. Raizer (2000), *Lightning Physics and Lightning Protection*, IoP Publishing Ltd.

C. P. Barrington-Leigh, U. S. Inan, and M. Stanley (2001), Identification of sprites and elves with intensified video and broadband array photometry, *J. Geophys. Res.,* 106(A2), 1741-1750, doi:/10.1029/2000ja000073.

D. J. Boccippio, E. R. Williams, S. J. Heckman, W. A. Lyons, I. T. Baker, and R. Boldi (1995), Sprites, ELF transients, and positive ground strokes, *Science,* 269, 1088--1091.

T. M. P. Briels, E. M. Van Veldhuizen, and U. Ebert (2008), Positive streamers in air and nitrogen of varying density: experiments on similarity laws, *J. Phys. D: Appl. Phys.,* 41(23), 234008.

O. Chanrion and T. Neubert (2008), A PIC-MCC code for simulation of streamer propagation in air, *J. Comput. Phys.,* 227, 7222-7245, doi:/10.1016/j.jcp.2008.04.016.

A. B. Chen, C.-L. Kuo, Y.-J. Lee, H.-T. Su, R.-R. Hsu, J.-L. Chern, H. U. Frey, S. B. Mende, Y. Takahashi, H. Fukunishi, Y. S. Chang, T.-Y. Liu, and L.-C. Lee (2008), Global distributions and occurrence rates of transient luminous events, *J. Geophys. Res.,* 113, A08306, doi:/10.1029/2008ja013101.

J. L. Chern, R. R. Hsu, H. T. Su, S. B. Mende, H. Fukunishi, Y. Takahashi, and L. C. Lee (2003), Global survey of upper atmospheric transient luminous events on the ROCSAT-2 satellite, *J. Atmos. Solar Terr. Phys.,* 65, 647--659, doi:/10.1016/s1364-6826(02)00317-6.

J. K. Chou, C. L. Kuo, L. Y. Tsai, A. B. Chen, H. T. Su, R. R. Hsu, S. A. Cummer, J. Li, H. U. Frey, S. B. Mende, Y. Takahashi, and L. C. Lee (2010), Gigantic jets with negative and positive polarity streamers, *J. Geophys. Res.,* 115, A00E45, doi:/10.1029/2009ja014831.

J. K. Chou, L. Y. Tsai, C. L. Kuo, Y. J. Lee, C. M. Chen, A. B. Chen, H. T. Su, R. R. Hsu, P. L. Chang, and L. C. Lee (2011), Optical emissions and behaviors of the blue starters, blue jets, and gigantic jets observed in the Taiwan transient luminous event ground campaign, *J. Geophys. Res.,* 116, A07301, doi:/10.1029/2010ja016162.

S. A. Cummer and U. S. Inan (1997), Measurement of charge transfer in sprite-producing lightning using ELF radio atmospherics, *Geophys. Res. Lett.,* 24(14), 1731-1734, doi:/10.1029/97gl51791.

S. A. Cummer, U. S. Inan, T. F. Bell, and C. P. Barrington-Leigh (1998), ELF radiation produced by electrical currents in sprites, *Geophys. Res. Lett.,* 25, 1281.

S. A. Cummer and M. Füllekrug (2001), Unusually intense continuing current in lightning causes delayed mesospheric breakdown, *Geophys. Res. Lett*., 28, 495–498. doi:10.1029/2000GL012214.

S. A. Cummer (2003), Current moment in sprite-producing lightning, *J. Atmos. Sol.-Terr. Phys.,* 65, 499-508.

S. A. Cummer and W. A. Lyons (2005), Implication of lightning charge moment changes for sprite initiation, *J. Geophys. Res.,* 110, A04304, doi:/10.1029/2004ja010812.

S. A. Cummer, N. C. Jaugey, J. B. Li, W. A. Lyons, T. E. Nelson, and E. A. Gerken (2006), Submillisecond imaging of sprite development and structure, *Geophys. Res. Lett.,* 33, L04104, doi:/10.1029/2005gl024969.

S. A. Cummer, J. Li, F. Han, G. Lu, N. Jaugey, W. A. Lyons, and T. E. Nelson (2009), Quantification of the troposphere-to-ionosphere charge transfer in a gigantic jet, *Nat. Geosci.,* 2, 617-620, doi:/10.1038/ngeo607.

S. A. Cummer, W. A. Lyons, and M. A. Stanley (2013), Three years of lightning impulse charge moment change measurements in the United States, *J. Geophys. Res.,* 118, 5176-5189, doi:/10.1002/jgrd.50442.

C. L. da Silva and V. P. Pasko (2012), Simulation of leader speeds at gigantic jet altitudes, *Geophys. Res. Lett.,* 39, 13805, L13805, doi:/10.1029/2012gl052251.

C. L. da Silva and V. P. Pasko (2013a), Vertical structuring of gigantic jets, *Geophys. Res. Lett.*, 40, 3315–3319.

C. L. da Silva and V. P. Pasko (2013b), Dynamics of streamer-to-leader transition at reduced air densities and its implications for propagation of lightning leaders and gigantic jets, *J. Geophys. Res.*, 118, 13561-13590.

C. L. da Silva and V. P. Pasko (2014), Infrasonic acoustic waves generated by fast air heating in sprite cores, *Geophys. Res. Lett.,* 41, 1789–1795, doi:10.1002/2013GL059164.

S. de Larquier and V. P. Pasko (2010), Mechanism of inverted-chirp infrasonic radiation from sprites, *Geophys. Res. Lett.,* 37, L24803, doi:/10.1029/2010gl045304.

U. Ebert, C. Montijn, T. M. P. Briels, W. Hundsdorfer, B. Meulenbroek, A. Rocco, and E. M. van Veldhuizen (2006), The multiscale nature of streamers, *Plasma Sources Sci. Technol.,* 15, S118-S129.

U. Ebert, W. van Saarloos, and C. Caroli (1997), Propagation and structure of planar streamer fronts, *Phys. Rev. E*, 55, 1530–1549, doi:10.1103/PhysRevE.55.1530.

U. Ebert and D. D. Sentman (2008), Editorial Review: Streamers, sprites, leaders, lightning: from micro- to macroscales, *J. Phys. D: Appl. Phys.,* 41(23), 230301, doi:/10.1088/0022-3727/41/23/230301.

U. Ebert, S. Nijdam, C. Li, A. Luque, T. Briels, and E. van Veldhuizen (2010), Review of recent results on streamer discharges and discussion of their relevance for sprites and lightning, *J. Geophys. Res.,* 115(A14), A00E43, doi:/10.1029/2009ja014867.

H. E. Edens (2011), Photographic and lightning mapping observations of a blue starter over a New Mexico thunderstorm, *Geophys. Res. Lett.,* 38, L17804, doi:/10.1029/2011gl048543.

T. Farges, E. Blanc, A. L. Pichon, T. Neubert, and T. H. Allin (2005), Identification of infrasound produced by sprites during the Sprite2003 campaign, *Geophys. Res. Lett.,* 32(1), L01813, doi:/10.1029/2004gl021212.

T. Farges and E. Blanc (2010), Characteristics of infrasound from lightning and sprites near thunderstorm areas, *J. Geophys. Res.,* 115, A00E31, doi:/10.1029/2009ja014700.

R. C. Franz, R. J. Nemzek, and J. R. Winckler (1990), Television image of a large upward electric discharge above a thunderstorm system, *Science,* 249, 48.

H. U. Frey, S. B. Mende, S. A. Cummer, J. Li, T. Adachi, H. Fukunishi, Y. Takahashi, A. B. Chen, R.-R. Hsu, H.-T. Su, and Y.-S. Chang (2007), Halos generated by negative cloud-to-ground lightning, *Geophys. Res. Lett.,* 34(18), L18801, doi:/10.1029/2007gl030908.

H. Fukunishi, Y. Takahashi, M. Kubota, K. Sakanoi, U. S. Inan, and W. A. Lyons (1996), Elves: Lightning-induced transient luminous events in the lower ionosphere, *Geophys. Res. Lett.,* 23(16), 2157--2160.

M. Füllekrug, D. R. Moudry, G. Dawes, and D. D. Sentman (2001), Mesospheric sprite current triangulation, *J. Geophys. Res.,* 106, 20189--20194.

M. Füllekrug, E. A. Mareev, and M. J. Rycroft (2006), *Sprites, elves and intense lightning discharges, NATO Science Series II: Mathematics, Physics and Chemistry*, vol. 225, Springer, Heidleberg, Germany.

M. Füllekrug, R. Roussel-Dupré, E. M. D. Symbalisty, O. Chanrion, A. Odzimek, O. van der Velde, and T. Neubert (2010), Relativistic runaway breakdown in low-frequency radio, *J. Geophys. Res.,* 115, 0, A00E09, doi:/10.1029/2009ja014468.

M. Füllekrug, R. Roussel-Dupré, E. M. D. Symbalisty, J. J. Colman, O. Chanrion, S. Soula, O. van der Velde, A. Odzimek, A. J. Bennett, V. P. Pasko, and T. Neubert (2011), Relativistic electron beams above thunderclouds, *Atmos. Chem. Phys.,* 11, 7747-7754, doi:/10.5194/acp-11-7747-2011.

M. Füllekrug, A. Mezentsev, S. Soula, O. van der Velde, and A. Evans (2013), Illumination of mesospheric irregularity by lightning discharge, *Geophys. Res. Lett.*, 40, 6411–6416, doi:10.1002/2013GL058502.

W. R. Gamerota, S. A. Cummer, J. Li, H. C. Stenbaek-Nielsen, R. K. Haaland, and M. G. McHarg (2011), Comparison of sprite initiation altitudes between observations and models, *J. Geophys. Res.,* 116, A02317, doi:/10.1029/2010ja016095.

E. A. Gerken, U. S. Inan, and C. P. Barrington-Leigh (2000), Telescopic imaging of sprites, *Geophys. Res. Lett.,* 27, 2637--2640.

E. A. Gerken and U. S. Inan (2002), A survey of streamer and diffuse glow dynamics observed in sprites using telescopic imagery, *J. Geophys. Res.,* 107(A11), 1344, doi:/10.1029/2002ja009248.

E. A. Gerken and U. S. Inan (2003), Observations of decameter-scale morphologies in sprites, *J. Atmos. Solar Terr. Phys.,* 65, 567--572, doi:/10.1016/s1364-6826(02)00333-4.

F. J. Gordillo-Vázquez (2008), Air plasma kinetics under the influence of sprites, *J. Phys. D: Appl. Phys.,* 41(23), 234016, doi:/10.1088/0022-3727/41/23/234016.

F. J. Gordillo-Vázquez and A. Luque (2010), Electrical conductivity in sprite streamer channels, *Geophys. Res. Lett.*, 37, L16809, doi:10.1029/2010GL044349.

F. J. Gordillo-Vázquez and A. Luque (2013), Preface to the Special Issue on Thunderstorm Effects in the Atmosphere-Ionosphere System, *Surv. Geophy.,* 34(6), 697-700, doi:/10.1007/s10712-013-9256-9.

C. Haldoupis, N. Amvrosiadi, B. R. T. Cotts, O. A. van der Velde, O. Chanrion, and T. Neubert (2010), More evidence for a one‐to‐one correlation between Sprites and Early VLF perturbations, J. Geophys. Res., 115, A07304, doi:10.1029/2009JA015165.

C. Haldoupis, M. Cohen, B. Cotts, E. Arnone, and U. Inan (2012), Long-lasting **D**-region ionospheric modifications, caused by intense lightning in association with elve and sprite pairs, *Geophys. Res. Lett.,* 39, L16801, doi:10.1029/2012GL052765.

L. C. J. Heijmans, S. Nijdam, E. M. van Veldhuizen, and U. Ebert (2013).

Streamers in air splitting into three branches. *EPL*, 103, 25002, doi:10.1209/0295-5075/103/25002.

R. H. Holzworth, M. C. Kelley, C. L. Siefring, L. C. Hale, and J. T. Mitchell (1985), Electrical measurements in the atmosphere and the ionosphere over an active thunderstorm. 2. Direct current electric fields and conductivity, *J. Geophys. Res.,* 90, 9824.

W. Y. Hu, S. A. Cummer, and W. A. Lyons (2007), Testing sprite initiation theory using lightning measurements and modeled electromagnetic fields, *J. Geophys. Res.,* 112, D13115, doi:/10.1029/2006jd007939.

S.-M. Huang, R.-R. Hsu, L.-J. Lee, H.-T. Su, C.-L. Kuo, C.-C. Wu, J.-K. Chou, S.-C. Chang, Y.-J. Wu, and A. B. Chen (2012), Optical and radio signatures of negative gigantic jets: Cases from Typhoon Lionrock (2010), *J. Geophys. Res.,* 117, A08307, doi:/10.1029/2012ja017600.

U. S. Inan, T. F. Bell, and J. V. Rodriguez (1991), Heating and ionization of the lower ionosphere by lightning, *Geophys. Res. Lett.,* 18, 705-708, doi:/10.1029/91gl00364.

U. S. Inan, W. A. Sampson, and Y. N. Taranenko (1996) Space-time structure of optical flashes and ionization changes produced by lighting-EMP, *Geophys. Res. Lett.,* 23(2), 133-136.

U. S. Inan, C. Barrington-Leigh, S. Hansen, V. S. Glukhov, T. F. Bell, and R. Rairden (1997), Rapid lateral expansion of optical luminosity in lightning-induced ionospheric flashes referred to as `elves', *Geophys. Res. Lett.,* 24(5), 583--586.

U. S. Inan, S. A. Cummer, and R. A. Marshall (2010), A survey of ELF and VLF research on lightning-ionosphere interactions and causative discharges, *J. Geophys. Res.,* 115, A00E36, doi:/10.1029/2009ja014775.

T. Kanmae, H. C. Stenbaek-Nielsen, and M. G. McHarg (2007), Altitude resolved sprite spectra with 3 ms temporal resolution, *Geophys. Res. Lett.,* 34, L07810, doi:10.1029/2006GL028608.

T. Kanmae, H. C. Stenbaek-Nielsen, M. G. McHarg, and R. K. Haaland (2010), Observation of sprite streamer head's spectra at 10,000 fps, J. Geophys. Res., 115, A00E48, doi:10.1029/2009JA01454.

T. Kanmae, H. C. Stenbaek-Nielsen, M. G. McHarg, and R. K. Haaland (2012), Diameter-speed relation of sprite streamers, *J. Phys. D: Appl. Phys.,* 45(26), 275203, doi:/10.1088/0022-3727/45/27/275203.

B. C. Kosar, N. Y. Liu, and H. K. Rassoul (2012), Luminosity and propagation characteristics of sprite streamers initiated from small ionospheric disturbances at subbreakdown conditions, *J. Geophys. Res.,* 117(A16), 8328, A08328, doi:/10.1029/2012ja017632.

B. C. Kosar, N. Y. Liu, and H. K. Rassoul (2013), Formation of sprite streamers at subbreakdown conditions from ionospheric inhomogeneities resembling observed sprite halo structures, *Geophys. Res. Lett., Geophys. Res. Lett.,* 40, 6282–6287, doi:10.1002/2013GL058294.

P. R. Krehbiel, J. A. Riousset, V. P. Pasko, R. J. Thomas, W. Rison, M. A. Stanley, and H. E. Edens (2008), Upward electrical discharges from thunderstorms, *Nat. Geosci.,* 1, 233--237, doi:/10.1038/ngeo162.

C. L. Kuo, R. R. Hsu, H. T. Su, A. B. Chen, L. C. Lee, S. B. Mende, H. U. Frey, H. Fukunishi, and Y. Takahashi (2005), Electric fields and electron energies inferred from the ISUAL recorded sprites, *Geophys. Res. Lett.,* 32, L19103, doi:/10.1029/2005gl023389.

C. L. Kuo, A. B. Chen, Y. J. Lee, L. Y. Tsai, R. K. Chou, R. R. Hsu, H. T. Su, L. C. Lee, S. A. Cummer, H. U. Frey, S. B. Mende, Y. Takahashi, and H. Fukunishi (2007), Modeling elves observed by FORMOSAT-2 satellite, *J. Geophys. Res.,* 112(A11), A11312, doi:/10.1029/2007ja012407.

C. L. Kuo, J. K. Chou, L. Y. Tsai, A. B. Chen, H. T. Su, R. R. Hsu, S. A. Cummer, H. U. Frey, S. B. Mende, Y. Takahashi, and L. C. Lee (2009), Discharge processes, electric field, and electron energy in ISUAL-recorded gigantic jets, *J. Geophys. Res.,* 114(A13), A04314, doi:/10.1029/2008ja013791.

A. S. Kyuregyan (2012), Transverse instability of a plane front of fast impact ionization waves, *J. Exp. Theor. Phys.*, 114 (5), 857–866, doi:10.1134/S1063776112030168.

J. Li, S. A. Cummer, W. A. Lyons, and T. E. Nelson (2008), Coordinated analysis of delayed sprites with high-speed images and remote electromagnetic fields, *J. Geophys. Res.,* 113(D12), D20206, doi:/10.1029/2008jd010008.

J. Li and S. A. Cummer (2009), Measurement of sprite streamer acceleration and deceleration, *Geophys. Res. Lett.,* 36, L10812, doi:/10.1029/2009gl037581.

J. Li and S. Cummer (2011), Estimation of electric charge in sprites from optical and radio observations, *J. Geophys. Res.,* 116, A01301, doi:/10.1029/2010ja015391.

J. Li, S. A. Cummer, G. Lu, and L. Zigoneanu (2012), Charge moment change and lightning-driven electric fields associated with negative sprites and halos, *J. Geophys. Res.,* 117(A9), A09310, doi:/10.1029/2012JA017731.

L. Liszka (2004), On the possible infrasound generation by sprites, *J. Low Freq. Noise, Vibration and Active Cont.,* 23(2), 85--93.

N. Y. Liu and V. P. Pasko (2004), Effects of photoionization on propagation and branching of positive and negative streamers in sprites, *J. Geophys. Res.,* 109, A04301, doi:/10.1029/2003ja010064.

N. Y. Liu, V. P. Pasko, D. H. Burkhardt, H. U. Frey, S. B. Mende, H.-T. Su, A. B. Chen, R.-R. Hsu, L.-C. Lee, H. Fukunishi, and Y. Takahashi (2006), Comparison of results from sprite streamer modeling with spectrophotometric measurements by ISUAL instrument on FORMOSAT-2 satellite, *Geophys. Res. Lett.,* 33, L01101, doi:/10.1029/2005gl024243.

N. Y. Liu and V. P. Pasko (2007), Modeling studies of NO-γ emissions of sprites, *Geophys. Res. Lett.,* 34, L16103, doi:/10.1029/2007gl030352.

N. Y. Liu, V. P. Pasko, K. Adams, H. C. Stenbaek-Nielsen, and M. McHarg

(2009a), Comparison of acceleration, expansion and brightness of sprite streamers obtained from modeling and high-speed video observations, *J. Geophys. Res,* 114, A00E03, doi:/10.1029/2008ja013720.

N. Y. Liu, V. P. Pasko, H. U. Frey, S. B. Mende, H.-T. Su, A. B. Chen, R.-R. Hsu, and L.-C. Lee (2009b), Assessment of sprite initiating electric fields and quenching altitude of $a^1\Pi_g$ state of N_2 using sprite streamer modeling and ISUAL spectrophotometric measurements, *J. Geophys. Res,* 114, A00E02, doi:/10.1029/2008ja013735.

N. Y. Liu (2010), Model of sprite luminous trail caused by increasing streamer current, *Geophys. Res. Lett.,* 37, L04102, doi:/10.1029/2009gl042214.

N. Y. Liu and V. P. Pasko (2010), NO-γ emissions from streamer discharges: direct electron impact excitation versus resonant energy transfer, *J. Phys. D: Appl. Phys.,* 43(8), 082001, doi:/10.1088/0022-3727/43/8/082001.

N. Y. Liu (2012), Multiple ion species fluid modeling of sprite halos and the role of electron detachment of O^- in their dynamics, *J. Geophys. Res,* 117, A03308, doi:/10.1029/2011ja017062.

N. Y. Liu (2014), Upper atmospheric electrical discharges, in The Lightning Flash, edited by V. Cooray, 2nd ed., pp. 725-786, The Institution of Engineering and Technology, London, UK.

N. Y. Liu, B. Kosar, S. Sadighi, J. R. Dwyer, and H. K. Rassoul (2012), Formation of streamer discharges from an isolated ionization column at subbreakdown conditions, *Phys. Rev. Lett.,* 109(2), 025002, doi:/10.1103/physrevlett.109.025002.

N. Y. Liu, J. R. Dwyer, H. C. Stenbaek-Nielsen, and M. G. McHarg (2014), Initiation of sprite streamers from natural mesospheric structures, Abstract AE34A-06 presented at 2014 Fall Meeting, AGU, San Francisco, Calif., 15-19 Dec.

N. Y. Liu, N. Spiva, J. R. Dwyer, H. K. Rassoul, D. Free, and S. A. Cummer. Upward electrical discharges observed above Tropical Depression Dorian (2015), *Nat. Commun*, 6:5995 doi: 10.1038/ncomms6995.

G. Lu, S. A. Cummer, W. A. Lyons, P. R. Krehbiel, J. Li, W. Rison, R. J. Thomas, H. E. Edens, M. A. Stanley, W. Beasley, D. R. MacGorman, O. A. van der Velde, M. B. Cohen, T. J. Lang, and S. A. Rutledge (2011), Lightning development associated with two negative gigantic jets, *Geophys. Res. Lett.,* 38, L12801, doi:/10.1029/2011gl047662.

A. Luque and U. Ebert (2009), Emergence of sprite streamers from screening-ionization waves in the lower ionosphere, *Nat. Geosci.,* 2(11), 757-760, doi:/10.1038/ngeo662.

A. Luque and U. Ebert (2010), Sprites in varying air density: Charge conservation, glowing negative trails and changing velocity, *Geophys. Res. Lett.,* 37, L06806, doi:/10.1029/2009gl041982.

A. Luque and U. Ebert (2011), Electron density fluctuations accelerate the branching of positive streamer discharges in air, *Phys. Rev. E,* 84(4), 046411.

A. Luque and F. J. Gordillo-Vázquez (2011), Sprite beads originating from inhomogeneities in the mesospheric electron density, *Geophys. Res. Lett.,* 38, L04808, doi:/10.1029/2010gl046403.

A. Luque and F. J. Gordillo-Vázquez (2012), Mesospheric electric breakdown and delayed sprite ignition caused by electron detachment, *Nat. Geosci.,* 5, 22-25, doi:/10.1038/ngeo1314.

W. A. Lyons (1996), Sprite observations above the U.S. High Plains in relation to their parent thunderstorm systems, *J. Geophys. Res.,* 101, 29641–29652.

W. A. Lyons, R. A. Armstrong, E. A. Bering, and E. R. Williams (2000), The hundred year hunt for the sprite, EOS Trans. Am. Geophys. Union 81, 373–377.

W. A. Lyons, T. E. Nelson, R. A. Armstrong, V. P. Pasko, and M. A. Stanley (2003), Upward electrical discharges from thunderstorm tops, *Bull. Am. Meteorol. Soc.,* 84(4), 445--454, doi:/10.1175/bams-84-4-445.

W. A. Lyons (2006), The meteorology of transient luminous events - An introduction and overview, in *Sprites, Elves and Intense Lightning Discharges, NATO Science Series II: Mathematics, Physics and Chemistry*, vol. 225, edited by M. Füllekrug, E. A. Mareev, and M. J. Rycroft, pp. 253–311, Springer, Heidleberg, Germany.

R. A. Marshall and U. S. Inan (2005), High-speed telescopic imaging of sprites, *Geophys. Res. Lett.,* 32, L05804, doi:/10.1029/2004gl021988.

R. A. Marshall, U. S. Inan, and V. S. Glukhov (2010), Elves and associated electron density changes due to cloud-to-ground and in-cloud lightning discharges, *J. Geophys. Res.,* 115, A00E17, doi:/10.1029/2009ja014469.

R. A. Marshall (2012), An improved model of the lightning electromagnetic field interaction with the d-region ionosphere, *J. Geophys. Res.,* 117, A03316, doi:/10.1029/2011ja017408.

M. G. McHarg, R. K. Haaland, D. R. Moudry, and H. C. Stenbaek-Nielsen (2002), Altitude-time development of sprites, *J. Geophys. Res.,* 107(A11), 1364, doi:/10.1029/2001ja000283.

M. G. McHarg, H. C. Stenbaek-Nielsen, and T. Kammae (2007), Streamer development in sprites, *Geophys. Res. Lett.,* 34, L06804, doi:/10.1029/2006gl027854.

M. G. McHarg, H. C. Stenbaek-Nielsen, T. Kanmae, and R. K. Haaland (2010), Streamer tip splitting in sprites, *J. Geophys. Res.,* 115, A00E53, doi:/10.1029/2009ja014850.

S. B. Mende, H. U. Frey, R. R. Hsu, H. T. Su, A. B. Chen, L. C. Lee, D. D. Sentman, Y. Takahashi, and H. Fukunishi (2005), D region ionization by lightning-induced EMP, *J. Geophys. Res.,* 110, A11312, doi:/10.1029/2005ja011064.

S. B. Mende, Y. S. Chang, A. B. Chen, H. U. Frey, H. Fukunishi, S. P. Geller, S. Harris, H. Heetderks, R. R. Hsu, L. C. Lee, H. T. Su, and Y. Takahashi (2006), Spacecraft based studies of transient luminous events, in *Sprites, Elves and Intense Lightning Discharges, NATO Science Series II: Mathematics*, Physics and Chemistry, vol. 225, edited by M. Füllekrug, E. A. Mareev, and M. J. Rycroft, pp. 123–149, Springer, Heidleberg, Germany.

T. C. Meyer, T. J. Lang, S. A. Rutledge, W. A. Lyons, S. A. Cummer, G. Lu, and D. T. Lindsey (2013), Radar and lightning analyses of gigantic jet-producing storms, *J. Geophys. Res. Atmos.,* 118, doi:10.1002/jgrd.50302.

R. Miyasato, M. J. Taylor, H. Fukunishi, and H. C. Stenbaek-Nielsen (2002), Statistical characteristics of sprite halo events using coincident photometric and imaging data, *Geophys. Res. Lett.,* 29(21), 2033, doi:/10.1029/2001gl014480.

J. Montanyà, O. van der Velde, D. Romero, V. March, G. Solà, N. Pineda, M. Arrayas, J. L. Trueba, V. Reglero, and S. Soula (2010), High-speed intensified video recordings of sprites and elves over the western Mediterranean Sea during winter thunderstorms, *J. Geophys. Res.,* 115, A00E18, doi:10.1029/2009JA014508.

R. C. Moore, C. P. Barrington-Leigh, U. S. Inan, and T. F. Bell, Early/fast VLF events produced by electron density changes associated with sprite halos, J. Geophys. Res., 108(A10), 1363, doi:10.1029/2002JA009816, 2003.

D. R. Moudry, H. C. Stenbaek-Nielsen, D. D. Sentman, and E. M. Wescott (2002), Velocities of sprite tendrils, *Geophys. Res. Lett.,* 29(20), 1992, doi:/10.1029/2002gl015682.

D. R. Moudry, H. C. Stenbaek-Nielsen, D. D. Sentman, and E. M. Wescott (2003), Imaging of elves, halos and sprite initiation at 1 ms time resolution, *J. Atmos. Solar Terr. Phys.,* 65, 509--518, doi:/10.1016/s1364-6826(02)00323-1.

T. Neubert (2003), On sprites and their exotic kin, *Science,* 300, 747-749.

T. Neubert, M. Rycroft, T. Farges, E. Blanc, O. Chanrion, E. Arnone, A. Odzimek, N. Arnold, C.-F. Enell, E. Turunen, T. Bösinger, Á. Mika, C. Haldoupis, R. J. Steiner, O. van der Velde, S. Soula, P. Berg, F. Boberg, P. Thejll, B. Christiansen, M. Ignaccolo, M. Füllekrug, P. T. Verronen, J. Montanya, and N. Crosby (2008), Recent Results from Studies of Electric Discharges in the Mesosphere, *Surv. Geophy.,* , doi:/10.1007/s10712-008-9043-1.

T. Neubert and O. Chanrion (2013), On the electric breakdown field of the mesosphere and the influence of electron detachment, *Geophys. Res. Lett.,* , doi:/10.1002/grl.50433.

R. T. Newsome and U. S. Inan (2010), Free-running ground-based photometric array imaging of transient luminous events, *J. Geophys. Res.,* 115, A00E41, doi:/10.1029/2009ja014834.

S. Nijdam, J. Moerman, T. Briels, E. van Veldhuizen, and U. Ebert (2008), Stereo-photography of streamers in air, *Appl. Phys. Lett.*, 92, 101502, doi:10.1063/1.2894195.

S. Nijdam, C. G. C. Geurts, E. M. van Veldhuizen, and U. Ebert (2009), Reconnection and merging of positive streamers in air, *J. Phys. D: Appl. Phys.,* 42, 045201.

M. M. Nudnova and A. Yu Starikovskii (2008), Streamer head structure: role of ionization and photoionization, *J. Phys. D: Appl. Phys.*, 41, 234003, doi:10.1088/0022-3727/41/23/234003.

V. P. Pasko, U. S. Inan, T. F. Bell, and Y. N. Taranenko (1997), Sprites produced by quasi-electrostatic heating and ionization in the lower ionosphere, *J. Geophys. Res.,* 102(A3), 4529--4561, doi:/10.1029/96ja03528.

V. P. Pasko, U. S. Inan, and T. F. Bell (1998), Spatial structure of sprites, *Geophys. Res. Lett.,* 25, 2123--2126.

V. P. Pasko and H. C. Stenbaek-Nielsen (2002), Diffuse and streamer regions of sprites, *Geophys. Res. Lett.,* 29(10), 1440, doi:/10.1029/2001gl014241.

V. P. Pasko, M. A. Stanley, J. D. Matthews, U. S. Inan, and T. G. Wood (2002), Electrical discharge from a thundercloud top to the lower ionosphere, *Nature,* 416, 152--154, doi:/10.1038/416152a.

V. P. Pasko (2003), Electric jets, *Nature,* 423, 927--929.

V. P. Pasko (2006), Theoretical modeling of sprites and jets, in *Sprites, Elves and Intense Lightning Discharges, NATO Science Series II: Mathematics, Physics and Chemistry*, vol. 225, edited by M. Füllekrug, E. A. Mareev, and M. J. Rycroft, pp. 253–311, Springer, Heidleberg, Germany.

V. P. Pasko (2007), Red sprite discharges in the atmosphere at high altitude: the molecular physics and the similarity with laboratory discharges, *Plasma Sources*

Sci. Technol., 16, S13-S29, doi:/10.1088/0963-0252/16/1/s02.

V. P. Pasko (2008), Blue jets and gigantic jets: transient luminous events between thunderstorm tops and the lower ionosphere, *Plasma Phys. Control. Fusion,* 50, 124050, doi:/10.1088/0741-3335/50/12/124050.

V. P. Pasko (2009), Mechanism of lightning-associated infrasonic pulses from thunderclouds, *J. Geophys. Res.,* 114, D08205, doi:/10.1029/2008jd011145.

V. P. Pasko (2010), Recent advances in theory of transient luminous events, *J. Geophys. Res.,* 115, A00E35, doi:/10.1029/2009ja014860.

V. P. Pasko, Y. Yair, and C.-L. Kuo (2011), Lightning related transient luminous events at high Altitude in the Earth's atmosphere: phenomenology, mechanisms and effects, *Space Sci. Rev.,* 168, 475-516, doi:/10.1007/s11214-011-9813-9.

V. P. Pasko, J. Qin, and S. Celestin (2013), Toward better understanding of sprite streamers: initiation, morphology, and polarity asymmetry, *Surv. Geophy.,* 34, 797-830, doi:/10.1007/s10712-013-9246-y.

N. I. Petrov and G. N. Petrova (1999), Physical mechanisms for the development of lightning discharges between a thundercloud and the ionosphere, *Tech. Phys.,* 44, 472-475, doi:/10.1134/1.1259327.

J. Qin, S. Célestin, and V. P. Pasko (2011), On the inception of streamers from sprite halo events produced by lightning discharges with positive and negative polarity, *J. Geophys. Res.,* 116, A06305, doi:/10.1029/2010ja016366.

J. Qin, S. Célestin, and V. P. Pasko (2012a), Formation of single and double-headed streamers in sprite-halo events, *Geophys. Res. Lett.,* 39, 5810, L05810, doi:/10.1029/2012gl051088.

J. Qin, S. Célestin, and V. P. Pasko (2012b), Minimum charge moment change in positive and negative cloud to ground lightning discharges producing sprites, *Geophys. Res. Lett.,* 39, 22801, L22801, doi:/10.1029/2012gl053951.

J. Qin, S. Célestin, and V. P. Pasko (2013), Dependence of positive and negative sprite morphology on lightning characteristics and upper atmospheric ambient conditions, *J. Geophys. Res.,* 118, 2623--2638, doi:/10.1029/2012ja017908.

J. Qin, V. P. Pasko, M. G. McHarg, and H. C. Stenbaek-Nielsen (2014), Plasma irregularities in the D-region ionosphere in association with sprite streamer initiation, Nat. Comm., 5, 3740.

Y. P. Raizer, G. M. Milikh, and M. N. Shneider (2006), On the mechanism of blue jet formation and propagation, *Geophys. Res. Lett.,* 33, L23801, doi:/10.1029/2006gl027697.

Y. P. Raizer, G. M. Milikh, and M. N. Shneider (2007), Leader streamers nature of blue jets, *J. Atmos. Sol.-Terr. Phys.,* 69, 925-938, doi:/10.1016/j.jastp.2007.02.007.

V. A. Rakov and M. A. Uman (2003), *Lightning: Physics and Effects*, Cambridge University Press, Cambridge, U.K.; New York.

J. A. Riousset, V. P. Pasko, P. R. Krehbiel, W. Rison, and M. A. Stanley (2010a), Modeling of thundercloud screening charges: Implications for blue and gigantic jets, *J. Geophys. Res.,* 115, A00E10, doi:/10.1029/2009ja014286.

J. A. Riousset, V. P. Pasko, and A. Bourdon (2010b), Air-density-dependent model for analysis of air heating associated with streamers, leaders, and transient luminous events, *J. Geophys. Res.,* 115, A12321, doi:/10.1029/2010ja015918.

W. Rison, R. J. Thomas, P. R. Krehbiel, T. Hamlin, and J. Harlin (1999), A GPS-based three-dimensional lightning mapping system: Initial observations in central New Mexico, *Geophys. Res. Lett.,* 26(23), 3573--3576, doi:/10.1029/1999gl010856.

A. Rocco, U. Ebert, and W. Hundsdorfer (2002), Branching of negative streamers in free flight, *Phys. Rev. E*, 66, 035102(R), doi:10.1103/PhysRevE.66.035102.

S. Sadighi, N. Y. Liu, J. R. Dwyer, and H. K. Rassoul (2015), Streamer formation and branching from model hydrometeors in subbreakdown conditions inside thunderclouds, *J. Geophys. Res.*, in review.

L. Savel'eva, A. Samusenko, and Y. K. Stishkov (2013), Reasons for branching of a positive streamer in a non-uniform field, *Surf. Eng. and Appl. Electrochem.*, 49(2), 125–135.

D. D. Sentman, E. M. Wescott, D. L. Osborne, D. L. Hampton, and M. J. Heavner (1995), Preliminary results from the Sprites94 campaign: red sprites, *Geophys. Res. Lett.,* 22, 1205--1208.

D. D. Sentman, H. C. Stenbaek-Nielsen, M. G. McHarg, and J. S. Morrill (2008), Plasma chemistry of sprite streamers, *J. Geophys. Res.,* 113, D11112, doi:/10.1029/2007jd008941.

D. D. Sentman (2010), Special Section: Effects of thunderstorms and lightning in the upper atmosphere, *J. Geophys. Res.,* http://onlinelibrary.wiley.com/journal/10.1002/(ISSN)2169-9402/specialsection/THUNDER1.

S. Soula, O. van der Velde, J. Montanya, P. Huet, C. Barthe, and J. Bór (2011), Gigantic jets produced by an isolated tropical thunderstorm near Réunion Island, *J. Geophys. Res.,* 116(D15), D19103, doi:/10.1029/2010jd015581.

M. Stanley, P. Krehbiel, M. Brook, C. Moore, W. Rison, and B. Abrahams (1999), High speed video of initial sprite development, *Geophys. Res. Lett.,* 26, 3201--3204.

H. C. Stenbaek-Nielsen, D. R. Moudry, E. M. Wescott, D. D. Sentman, and F. T. S. Ao Sabbas (2000), Sprites and possible mesospheric effects, *Geophys. Res. Lett.,* 27, 3829--3832.

H. C. Stenbaek-Nielsen, M. G. McHarg, T. Kammae, and D. D. Sentman (2007), Observed emission rates in sprite streamer heads, *Geophys. Res. Lett.,* 34, L11105, doi:/10.1029/2007gl029881.

H. C. Stenbaek-Nielsen and M. G. McHarg (2008), High time-resolution sprite imaging: observations and implications, *J. Phys. D: Appl. Phys.,* 41(23), 234009, doi:/10.1088/0022-3727/41/23/234009.

H. C. Stenbaek-Nielsen, R. Haaland, M. G. McHarg, B. A. Hensley, and T. Kanmae (2010), Sprite initiation altitude measured by triangulation, *J. Geophys. Res.,* 115, A00E12, doi:/10.1029/2009ja014543.

H. C. Stenbaek-Nielsen, T. Kanmae, M. G. McHarg, and R. Haaland (2013), High-Speed Observations of Sprite Streamers, *Surv. Geophys.,* 34, 769--795, doi:/10.1007/s10712-013-9224-4.

H. T. Su, R. R. Hsu, A. B. Chen, Y. C. Wang, W. S. Hsiao, W. C. Lai, L. C. Lee, M. Sato, and H. Fukunishi (2003), Gigantic jets between a thundercloud and the ionosphere, *Nature,* 423, 974--976, doi:/10.1038/nature01759.

A. B. Sun, J. Teunissen, and U. Ebert (2013), Why isolated streamer discharges hardly exist above the breakdown field in atmospheric air, *Geophys. Res. Lett.,* 40, 2417-2422, doi:10.1002/grl.50457.

T. Suzuki, M. Hayakawa, Y. Hobara, and K. Kusunoki (2012), First detection of summer blue jets and starters over Northern Kanto area of Japan: Lightning activity, *J. Geophys. Res.,* 117, A07307, doi:/10.1029/2011ja017366.

M. J. Taylor, M. A. Bailey, P. D. Pautet, S. A. Cummer, N. Jaugey, J. N. Thomas, N. N. Solorzano, F. S. Sabbas, R. H. Holzworth, O. Pinto, and N. J. Schuch (2008), Rare measurements of a sprite with halo event driven by a negative lightning discharge over Argentina, *Geophys. Res. Lett.,* 35, L14812, L14812, doi:/10.1029/2008gl033984.

O. A. van der Velde, W. A. Lyons, T. E. Nelson, S. A. Cummer, J. Li, and J.

Bunnell (2007), Analysis of the first gigantic jet recorded over continental North America, *J. Geophys. Res.,* 112, D20104, doi:/10.1029/2007jd008575.

O. A. van der Velde, J. Bór, J. Li, S. A. Cummer, E. Arnone, F. Zanotti, M. Füllekrug, C. Haldoupis, S. Naitamor, and T. Farges (2010), Multi-instrumental observations of a positive gigantic jet produced by a winter thunderstorm in Europe, *J. Geophys. Res.,* 115(D14), D24301, doi:/10.1029/2010jd014442.

J. R. Wait and K. P. Spies (1964), Characteristics of the Earth-ionosphere waveguide for VLF radio waves, *Tech. Note 300,* Natl. Bur. of Stand., Boulder, Colo., 30 Dec.

E. M. Wescott, D. Sentman, D. Osborne, D. Hampton, and M. Heavner (1995), Preliminary results from the Sprites94 aircraft campaign: 2. Blue jets, *Geophys. Res. Lett.,* 22(10), 1209--1212.

E. M. Wescott, D. D. Sentman, M. J. Heavner, D. L. Hampton, D. L. Osborne, and O. H. Vaughan Jr. (1996), Blue starters: Brief upward discharges from an intense Arkansas thunderstorm, *Geophys. Res. Lett.,* 23(16), 2153--2156, doi:/10.1029/96gl01969.

E. M. Wescott, D. D. Sentman, M. J. Heavner, D. L. Hampton, and O. H. Vaughan Jr. (1998), Blue jets: their relationship to lightning and very large hailfall, and their physical mechanisms for their production, *J. Atmos. Solar Terr. Phys.,* 60, 713--724.

E. M. Wescott, D. D. Sentman, H. C. Stenbaek-Nielsen, P. Huet, M. J. Heavner, and D. R. Moudry (2001a), New evidence for the brightness and ionization of blue starters and blue jets, *J. Geophys. Res.,* 106, 21549-21554, doi:/10.1029/2000ja000429.

E. M. Wescott, H. C. Stenbaek-Nielsen, D. D. Sentman, M. J. Heavner, D. R. Moudry, and F. T. S. Sabbas (2001b), Triangulation of sprites, associated halos and their possible relation to causative lightning and micrometeors, *J. Geophys. Res.,* 106(A6), 10467--10478, doi:/10.1029/2000ja000182.

E. R. Williams (2006), Problems in lightning physics--the role of polarity asymmetry, *Plasma Sources Sci. Technol.,* 15(2), S91--S108, doi:/10.1088/0963-0252/15/2/s12.

E. Williams, E. Downes, R. Boldi, W. Lyons, and S. Heckman (2007), Polarity asymmetry of sprite-producing lightning: A paradox?, *Radio Sci.,* 42, RS2S17, doi:/10.1029/2006rs003488.

E. Williams, C.-L. Kuo, J. Bór, G. Sátori, R. Newsome, T. Adachi, R. Boldi, A. Chen, E. Downes, R. R. Hsu, W. Lyons, M. M. F. Saba, M. Taylor, and H. T. Su (2012), Resolution of the sprite polarity paradox: The role of halos, *Radio Sci.,* 47, RS2002, doi:/10.1029/2011rs004794.

C. T. R. Wilson (1925), The electric field of a thundercloud and some of its effects, *Proc. Phys. Soc. London,* 37(32D).

J. Yang and G. L. Feng (2012), A gigantic jet event observed over a thunderstorm in mainland china, *Chinese Science Bulletin,* 57(36), 4791-4800, doi:/10.1007/s11434-012-5486-3.

N. A. Zabotin and J. W. Wright (2001), Role of meteoric dust in sprite formation, *Geophys. Res. Lett.*, 28(13), 2593-2596, doi:10.1029/2000GL012699.